A decision support system tool to manage the flexibility in renewable energy-based power systems

Building and Environment 199 (2021) 107906

Contents lists available at ScienceDirect

Building and Environment

journal homepage: www.elsevier.com/locate/buildenv

Modelling double skin façades (DSFs) in whole-building energy simulation tools: Validation and inter-software comparison of a mechanically ventilated single-story DSF

Elena Catto Lucchino [a], Adrienn Gelesz [b,c], Kristian Skeie [a], Giovanni Gennaro [d,e], András Reith [b,f], Valentina Serra [d], Francesco Goia [a,*]

[a] Department of Architecture and Technology, Norwegian University of Science and Technology, NTNU, Trondheim, Norway
[b] Advanced Building and Urban Design Ltd, Budapest, Hungary
[c] Faculty of Architecture, Budapest University of Technology and Economics, Budapest, Hungary
[d] Department of Energy, Politecnico di Torino, Torino, Italy
[e] Institute for Renewable Energy, EURAC Research, Bolzano, Italy
[f] Faculty of Engineering and Information Technology, University of Pécs, Pécs, Hungary

ARTICLE INFO

Keywords:
Inter-software comparison
Model validation
EnergyPlus
TRNSYS
IDA ICE
IES VE

ABSTRACT

Double skin façades (DSFs) have been proposed as responsive building systems to improve the building envelope's performance. Reliable simulation of DSF performance is a prerequisite to support the design and implementation of these systems in real buildings. Building energy simulation (BES) tools are commonly used by practitioners to predict the whole building energy performance, but the simulation of the thermophysical behaviour of DSFs may be challenging when carried out through BES tools. Using an exhaust-air façade case study, we analyse and assess the reliability of four popular BES tools when these are used to simulate a DSF, either through available in-built models or through custom-built representations based on zonal models. We carry out this study by comparing numerical simulations and experimental data for a series of significant thermophysical quantities, and we reflect on the performance and limitations of the different tools. The results show that no tool is outstandingly better performing over the others, but some tools offer better predictions when the focus is placed on certain thermophysical quantities, while others should be chosen if the focus is on different ones. After comparing the different models' limitations and challenges, we conclude that BES tools can simulate the performance of DSF systems over long periods. However, their use alone is not recommended when the simulation's scope is to replicate and study short-term phenomena and dynamic aspects, such as sizing the building's HVAC system.

1. Introduction

Double skin façades (DSFs) are a typology of solar façades which are often adopted to reduce energy use [1] and to provide better thermal and visual comfort conditions compared to traditional single-skin façades [2]. Because of the more complicated behaviour than conventional building envelope solutions, the design and optimisation of a DSF cannot be based on rules-of-thumb or simple performance parameters. However, they should be based on results derived from dynamic energy performance simulation. A detailed simulation of the thermal, fluid mechanics and optical behaviour of a DSF can be obtained using different approaches, such as on-purpose built models [3–5] or dedicated CFD simulations [6,7]. However, the simulation of the DSF alone, without the integration into the building. limits to a great extent the possibility to study the DSF's performance under real operation. Building Energy Software (BES) tools are, on the other side, meant for modelling an entire building and predicting the whole building energy performance, and when a DSF is modelled in a BES tool, it is, therefore, possible to link the DSF's performance with that of the entire building. The coupled simulation of the whole building and the specific building components is essential for correctly assessing the overall energy and comfort performance. It is the only way to replicate the complex interaction between airflow in the façade, the HVAC system, and the building energy management system. There are indeed a series of studies where different BES tools have been used to evaluate the behaviour of DSFs

* Corresponding author.
E-mail address: francesco.goia@ntnu.no (F. Goia).

https://doi.org/10.1016/j.buildenv.2021.107906
Received 2 November 2020; Received in revised form 14 April 2021; Accepted 15 April 2021
Available online 23 April 2021

Nomenclature

ACH	ventilation rate (air changes per hour, 1/h)
ΔT	temperature difference (K)
g	solar factor (−)
h_c	convective heat transfer coefficient (W/(m^{2}K))
H	height of the window (m)
k	thermal conductivity of the fluid (W/(mK))
L	cavity width (m)
λ	thermal conductivity of air (W/mK)
M_i	measured value at one point
n	total number of measurements
Nu	Nusselt number (−)
P_i	simulated predicted value
Pr	Prandtl number (−)
Ra_H	Rayleigh number based on the height (−)
Re	Reynolds number (−)
ρ_{in}	glazing solar reflectance, inner face (−)
ρ_{out}	glazing solar reflectance, outer face (−)
τ	glazing solar transmittance (−)
U	thermal transmittance (W/(m^{2}K))
$\dot{V}$	airflow rate (m^3/s)
v	velocity (m/s)
$\bar{y}$	mean value of the measured values

[8–13]. BES tools have not been developed with the precise requirement to simulate an advanced building envelope system such as a DSF. Only a few BES tools include dedicated modules for DSFs' simulation, while it is more common that the modelling of these systems might require some workarounds or the use of relatively advanced simulation strategies [14].

The main aim of the research activity presented in this paper is to evaluate the capabilities and accuracy of some of the most commonly adopted BES tools in modelling a relatively common mechanically ventilated DSF type, called *climate façade*. In these façades, which can be single-storey or multiple-storey high, the air typically enters the façade cavity from the indoor environment in the lower region of the façade and leaves the cavity at the upper part of the façade extracted through a duct as part of the HVAC system [15]. This research's secondary aim is to highlight how current shortcomings in BES software programs regarding modelling and simulation of DSF systems should be addressed to improve the simulation tools' reliability.

Robust and comprehensive comparison and experimental validation of building performance simulation tools are common practices and have been carried out for commercially available BES tools. Often, standardised geometries and configurations, such as the IEA Building Energy Simulation Test and Diagnostic Method (IEA BESTEST) or the ANSI/ASHRAE Standard 140, are used to validate and verify different functions of BES tools, ranging from building systems and wall assemblies (e.g. Refs. [16,17]) to environmental systems (e.g. Refs. [18,19]). These procedures' objectives are to increase confidence in using BES tools and improve simulation engines' current generation. However, dedicated validation and verification activities targeting such tools' reliability in replicating DSF systems' performance are rare, even though DSFs are building envelope systems nowadays rather largely employed and frequently designed through BES tools [20]. More than ten years have passed since the only major inter-comparison of software tools [21] in modelling DSFs was performed. In that study, the empirical validation of a naturally ventilated DSF, when operated as an outdoor air curtain and when in "thermal buffer", was presented, while mechanically ventilated configurations were not addressed. The results showed that none of the models found in the software tools at that time produced consistent results if compared to the experimental data, especially in periods of higher solar intensity.

In this paper, we extend the preliminary work on the experimental validation of an exhaust-air façade model through comparison with experimental data from a test cell experiment [22], assessing and comparing the performance of different modelling approaches and models implemented in four different BES tools: EnergyPlus, IDA Indoor Climate and Energy (IDA ICE), IES Virtual Environment (IES VE), and TRNSYS. EnergyPlus [23] is a whole building energy simulation program used to model energy consumption—heating, cooling, ventilation, lighting and plug and process loads—and water use in buildings. It is a freeware software tool with a publicly available source code, which the user can modify to create an ad-hoc version to add simulation functions – which is not a trivial task. When it comes to possibilities to model DSF systems, Energy Plus has an in-built model called "Airflow Window", which has been used in a few studies for modelling a DSF [22,24]. Most of the studies adopt instead the so-called zonal approach [13,25–28], which also allows naturally ventilated cavities to be modelled (a possibility not allowed by the "Airflow Window" model). IDA ICE [29] is a licensed equation-based multi-zone simulation building program whose library is written in Neutral Model Format (NMF), a common format of model expression that allows users to interconnect different modules and develop sub-routines directly in the programming interface. The structure of IDA ICE allows easier on-demand modifications of the different models already implemented. IDA ICE, as EnergyPlus, includes an in-built component specifically developed to model DSFs called "Ventilated Window" [22]. Adopting multiple zone modelling based on the typical stacked thermal zones approach is always possible and seen in the literature, especially when modelling multi-storeys [30]. IES VE Virtual Environment [31] is a commercial software tool whose code is not accessible, limiting its application to models already included in the software's distributed version. Few examples of DSFs modelled as stacked thermal zones are available in the literature [10,32]. TRNSYS [33] is a commercial simulation code initially developed for solar thermal systems, which offers the possibility to model and simulate multi-zone buildings through a combined thermal and airflow network model. The use of this tool among researchers is well established, as it also allows the development of dedicated sub-routines in a relatively easy way. Multiple studies on DSFs are available in the literature, where the majority of them has covered naturally ventilated façades [34–41]. In a recent release of Trnsys 18, an inbuilt model called "Complex Fenestration System" was made available. Besides implementing an optical model based on the so-called "Bidirectional Scattering Distribution Function" (BSDF) to provide high-quality daylighting simulation for fenestrations equipped with slat systems or honeycomb structures, this component allows modelling mechanically ventilated gaps [42].

The investigation results of this study are meant for both the research and the practitioners' community and for building performance software developers, as they both unveil the reliability and challenges of modelling and simulating mechanically ventilated DSFs with current BES tools.

The article is organised as follows. In Section 2 – Methodology, we present the research activity's overall objectives, together with the different methods employed: ranging from the presentation of the case-study façade to the modelling implementation in BES tools, from experimental data collection and processing to the validation procedure. For the sake of readability, more details on the data for validation and the DSF's implementation for each BES tool are reported in Appendix A and Appendix B, respectively. In Section 3 – Results, we provide an extensive report of the validation and performance assessment outcomes for the different tools, based on several validation variables and periods/

conditions. We analyse the results in terms of individual thermophysical quantities and software performance under different boundary conditions. In Section 4 – Discussions, we reflect on our analysis results and highlight current limitations in the different tools that lead to inaccuracy in the performance prediction, while the conclusive summary of the paper is presented in Section 5 – Conclusions.

2. Methodology

The methodological approach to the research has been broken down in a series of steps that are described by the following objectives: i) to model, with different BES tools, a case study façade that can be representative of a relatively large number of mechanically ventilated façades; ii) to process data from a previous experimental analysis on the same type of DSF and prepare them for the use in the validation process, identifying a series of thermophysical quantities available in both the experimental dataset and the simulation outputs, and identifying a series of suitable periods characterised by different boundary conditions and operational modes; iii) to run the different BES tools' models for the DSF for a relatively long-time simulation run (two weeks for each period), using as input data the boundary conditions registered during the experiments; iv) to establish a suitable set of methods and performance metrics to compare the simulated and measured values, for the selected thermophysical quantities, through both a qualitative and quantitative approach; v) to analyse and quantify the performance of each simulation tool against the experimental data; vi) to understand the possible reasons for discrepancies between different software tools and between numerical and experimental data. The objectives i to iv are detailed in the next sections 2.1, 2.2, 2.3, and 2.4, respectively, while the last two objectives are presented in Section 3 and Section 4, respectively.

2.1. Numerical modelling in four BES tools

2.1.1. Case study façade

The DSF used in this investigation is a mechanically ventilated, single-story high DSF operated as a so-called *climate façade*. In climate façades, the air from the room enters the cavity at the bottom, flows through the cavity and is extracted at the top and directed to the HVAC system's air handling unit as a part of the ventilation network of the building. Therefore, the flow rate is usually linked to fresh air supply requirements rather than optimised to achieve a specific performance when it comes to the façade. A climate façade can guarantee a stable glass surface temperature (thus reducing the risk of thermal discomfort), remove a large share of the (potential) cooling loads due to the solar gains through the ventilation air, especially when a shading device is installed in the cavity, and reduce to a great extent the transmission heat loss due to the double glazed layer. Climate façades are among the most popular DSFs, and single-storey climate façades are solutions that assure a (relatively) simple construction, safety, and simpler operation – compared to multi-storey double-skin facades.

The specific façade in this study, as schematised in Fig. 1, was modelled to represent in the DSF that was experimentally tested (Fig. 3): dimensions 1.60 m (width) and 3.40 m (height), and a ventilated cavity of 0.24 m (depth), with a volumetric airflow of 20 m^3/h and hosting a highly reflective roller blind as a shading device, located 0.07 m from the external skin. The airflow enters the ventilated cavity from small openings in the frame at the bottom of the façade and a fan extracts the air from the cavity top through a duct. The shading installed in the cavity is placed at 7 cm from the external glazing, and while the airflow is not constrained in one of the two half-cavities created by the roller blind, there is no particular measure to assure that the airflow is evenly distributed between the two sides of the shading device.

The external skin of the DSF was made of an insulated glazed unit with two glass panes with a selective coating, and the internal skin was made of a single, clear glass pane. Most of the façades' thermal and optical properties were available from technical documentation. Simultaneously, a few data (related to the shading device) that was not wholly documented was assumed based on our experience and realistic

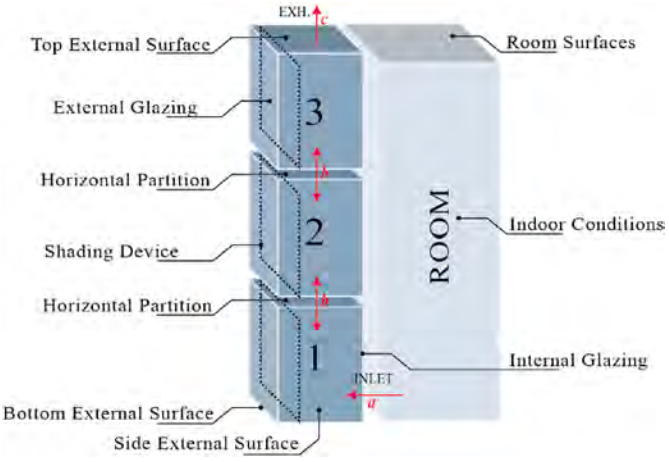

Fig. 2. Zonal modelling of the DSF.

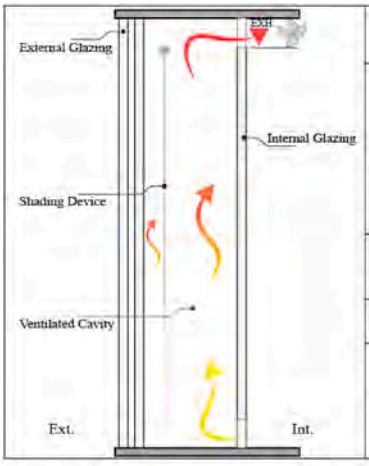

Layers from exterior to interior		Thickness [mm]	τ_{sol} [-]	ρ_{out} [-]	ρ_{in} [-]	U * [W/m²K]	g* [-]
External glazing	Laminated glass - selective coating, pos.2, 10.10.4	20	0.32	0.31	0.45	1.36	0.38
	Air	16					
	Clear glass	10					
Shading Device	High reflectance roller blind	1	0.10	0.80	0.80	-	-
Ventilated Cavity	Air	240	-	-	-	-	-
Internal glazing	Laminated clear glass 5.5.4	10	0.7	0.07	0.07	5.59	0.79

**At reference conditions defined by ISO 15099:2003.*

Fig. 1. Schematic section and glazing configuration of the DSF
*At reference conditions defined by ISO 15099:2003.

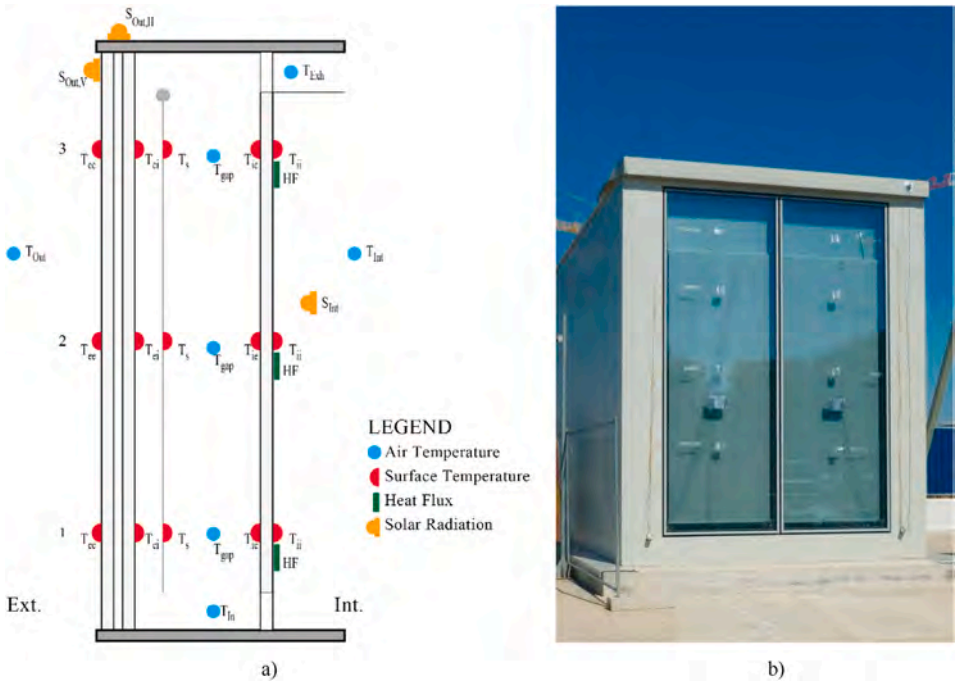

Fig. 3. Sensor a) scheme and b) instalment on the experiment facility.

hypothesis based on similar designs. The global solar optical and thermal properties of the glazing and shading have been calculated, based on the available information, using LBNL Window 7.7 and Optics 6 using the IGDB v29, and are reported in Fig. 1.

The geometrical, thermal, optical, and operational (airflow rate) features of the DSF have been implemented in different BES tools, according to the possibilities given by each software environment, as described in the next section.

2.2. DSF model implementation in BES tools

This study's primary goal is to compare the different modelling approaches and embedded modules available in some BES tools and evaluate their abilities to replicate the thermophysical and optical behaviour of mechanically ventilated DSFs. For this reason, the entire modelling and validation task focused on the case-study façade and the façade-related quantities (e.g. the thermophysical quantities linked to the façade alone, such as the air gap temperature, the surface temperatures, heat flux exchanged at the façade interface) and not on the environment and environment-related quantities (indoor air temperature, or energy for heating or cooling of the building behind the façade). The façade was modelled as belonging to one of the surfaces of a simple box-shaped thermal zone, whose constructional features—except for the DSF—were not of interest in this study. The other surfaces of the box's envelope were modelled as non-exposed surfaces (nor sun, nor wind exposure). Implementing the input data in the different simulation environments might require different strategies or methods, but we paid attention to be sure that, regardless of the actual way to implement certain information, the core of the modelling was kept identical in all the tools.

However, some differences can arise from each tool's processor engines outside the set of equations that describe the façade's optical and thermophysical behaviour. For example, the input data read from an hourly value and used to run a sub-hourly simulation, and then reported as hourly output. Moreover, each tool has different routines to treat solar data. During the daytime, the way solar radiation is treated in the different models may generate inaccuracy in the predictions that cannot be accounted to the modelling approach or the physical-mathematical description of the DSF, but rather to the overall simulation environment.

As described in full details in Appendix B, different approaches were used in the four selected tools to model the case-study façade. In general, it was possible to model the DSF either through available in-built modules (in EnergyPlus, IDA ICE, and Trnsys) or using the so-called zonal approach. In the latter modelling strategy, the cavity is divided into several thermal zones stacked one over the other. The zones are connected through an airflow network representation that allows one to describe the airflow through the different zones. Several authors explored the role of the number of stacked thermal zones on the quality and reliability of the simulation [9,43], but there is no consensus nor a standardised approach when it comes to this setting, which usually ranges (when referred to single-storey DSFs) from a minimum of one to a maximum of six [20]. A dedicated comparative analysis on models with one to six zones stacked upon each other showed that, in the case of a mechanically ventilated exhaust-air façade, an increase in the zones' number does not significantly affect the results [44]. For these reasons, we decided to model the DSF, when the zonal approach was used, with three stacked thermal zones (Fig. 2), which also corresponded to the experimental setup adopted for the measurement campaign that provided data for the validation – sensors were installed at three different levels of the façade's cavity, as explained more in details in Section 2.3. Table 1 and Table 2 describe the thermal and the airflow network models in the different BES tools.

We used our best knowledge as modellers of the different simulation environments and as building physicists about the thermophysical behaviour of the case study façade to provide the four BES tools with the same level of information about the DSF. We consciously decided not to calibrate the models on available experimental data. This approach is motivated by the fact that only through un-calibrated models it is possible to assess the simulation performance of the different tools during a hypothetical design phase – when experimental data on the solution under design are not available. Furthermore, only with un-calibrated models the reasons for mispredictions can potentially be unveiled. The choice to avoid any calibration to assess the "true" performance of the different BES might lead to inaccuracy in the simulation workflow due to a user error in place of a program error, as a calibration process can somehow "fix" a user error. In order to reduce the risk of a

Table 1
Thermal model of the DSF in the zonal approach.

	EnergyPlus	TRNSYS	IDA ICE	IES-VE
Horizontal Partition	Infrared material	Virtual surface	Adiabatic surface[a]	Hole
Top/Side/ Bottom External Surfaces	Adiabatic surface	Adiabatic surface	Adiabatic surface	Adiabatic surface
Room surfaces	Highly conductive surface with temperature on the other side assigned by a schedule	Temperature assigned by a schedule	Highly conductive surface with temperature on the other side assigned by a schedule	Highly conductive surface with temperature on the other side assigned by a schedule
Shading Device	Internal - Shade	Internal – Shading	Internal - Shade	Internal - Blind
Temperature Set-point	Ideal load	Ideal load	HVAC	HVAC

[a] See Appendix B, Modelling of DSF in IDA ICE.

Table 2
Airflow network connection in the zonal approach of the DSF.

		EnergyPlus	TRNSYS	IDA ICE	IES VE
a)	**Inlet**	Leak	Circular duct	Leak	Simple Opening
b)	**Horizontal Partition**	Horizontal Opening	Horizontal Opening	Horizontal Opening	Horizontal Opening
c)	**Exhaust**	Exhaust Fan	Circular duct	Exhaust Fan	Exhaust Fan

user error occurring, all the models implemented in the different tools have been revised multiple times by different modellers, thus assuring a redundant and independent check of the models' quality. Moreover, simulations have been run for more extended periods, using the typical meteorological year, and the simulation outputs from different tools screened in search of significant differences that are usually proof of user errors. However, as we know that user error can in practice be very difficult to avoid completely, we made available on an open-access repository the models used for this simulation study to allow easy replication and, potentially, a quality check of our results by the scientific community – see Appendix B.

We used, as far as possible, homogenous settings for the different general settings of the four simulation engines, and we did not implement particular changes in the different models that might derive by knowing in advance the performance of the façade used for this study. For example, we did not implement modifications in the algorithms for the calculation of the convective heat transfer coefficient in the cavity (which is a factor that might have an impact on the results of the simulation), and we relied on the implemented solutions available in the four simulation tools, selecting (where possible) the best option among those available. In some of the tools, the calculation method is an algorithm that chooses among different correlations as a function of the flow regime (Energy Plus) or the maximum value between two different correlations (IDA ICE); in some other, the choice that the user can make is only between using a constant value or a specific function implemented in the tool (IES-VE and Trnsys). The calculation methods to derive the convective coefficient for the internal (indoor) and external (outdoor) surfaces of the room have been set as displayed in Table 3. In the zonal approach, the same correlations are adopted for the surfaces of the DSF; when using the in-built models, specific correlations within those models are adopted. The convective correlations adopted for the ventilated cavity's vertical surfaces, as implemented in the different tools, are listed in Table 4.

Table 3
Calculation methods for establishing the exterior (outdoor) and interior (indoor) convective surface coefficients.

	External Surfaces	Internal Surfaces
EnergyPlus	*SimpleCombined* [23]	*AdaptiveConvectionAlgorithm* [23]
IDA ICE	*Clarks* [45]	max*(Table, CDA)* [46]
IES VE	*McAdams* [47]	*Alamdari & Hammond* [48]
TRNSYS	*Constant Value* [49]	*Constant Value*[a] [49]

[a] For the surfaces of the cavity, the Internal Calculation Method is selected (see Table 4).

2.3. Experimental data collection and validation of data processing

Two modules of the case-study DSF were continuously monitored for around two years using an outdoor test-cell facility (that replicated a full-scale office room) located in a temperate sub-continental climate location in northern Italy (45° N latitude). The DSF was installed on the 15° southwest exposed façade.

The room's indoor air temperature was set at 20 °C in winter and 26 °C in summer to minimise inaccuracies due to transient states in the indoor environment and ensure stable testing conditions. The test-cell and the DSF modules (Fig. 3) were equipped with a wide range of sensors (thermocouples for surface and air temperature measurements, heat flux meter sensors, pyranometers both inside and outside) to record the thermophysical and optical processes occurring in the DSF. Temperature and heat flux sensors were placed at three height levels, both inside and outside of the façade, measuring: the surface temperature of the interior glazing and the exterior glazing (both towards the indoor and the cavity); the surface temperature of the roller screen (towards the indoor glazing); the temperature of the air in the cavity behind the shading (when present); the inlet and outlet cavity-air temperature; the frame temperature; the heat flux exchanged at the indoor surface of the glazing. Thermocouples and heat flux meters directly exposed to solar radiation were shielded with highly reflecting aluminium foils to reduce solar irradiance's influence on the measured physical quantity, following best practices established in the literature [54]. Furthermore, the outdoor solar irradiance was measured both on the horizontal and vertical plane, employing two pyranometers. The solar irradiance transmitted through the DSF was measured, on the vertical plane, with an additional pyranometer installed right next to the inner skin of the DSF. The test-cell was also equipped with contact sensors to record the surface temperature values for all the cell's surface, as well as with sensors for indoor air temperature measurements.

The measurement accuracies for the entire measurement chain, after calibration and verification, were: ±0.3 °C, ±5% and ±5%, for thermocouples, heat flux meters, and pyranometers, respectively. More detailed information on the experimental campaign can be found in Refs. [22,55].

From the entire dataset of nearly two years of measurements, we selected for this validation study a series of weeks that could represent different operational conditions, different periods of the year, and different boundary conditions. DSF was operated with either the shading device deployed or retracted, with considerably different performance. For a validation purpose, it is interesting to investigate the performance at least in winter and in summer, and different conditions should be included in each of the seasons (sunny days and cloudy days, warm days and cold days) to test a broad spectrum of boundary conditions. Based on these considerations, four periods of two weeks each were selected, characterised by different weather conditions, so that two operational modes (with and without the shading device) can be combined with the two seasons. For each period, the first week was only used for modelling warm-up, while the second week was used for the actual validation process. Fig. 4 shows the main boundary conditions (outdoor and indoor air temperature and global irradiance on the horizontal plane) for the second week of each of the four periods. Due to limitations in the

Table 4
Convective heat transfer correlations adopted for the ventilated cavity's vertical surfaces.

Software	Calculation Method	Reference	Convective heat transfer coefficient model
EnergyPlus	Adaptive Convection Algorithm - Windows	ISO 15099 [50]	$h_{c,nat} = Nu*\frac{\lambda}{H}$ $Nu = f(Ra_H)$
		Goldstein -Novoselac [51]	$h_{c,forced} = 0.103\left(\frac{\dot{V}}{L}\right)^{0.8}$
EnergyPlus AW	Airflow window model	ISO 15099 [50]	$h_c = 2h_{c,\ enclosed\ gap} + 4v$
IDA ICE	max (Table, CDA)	$h_c = \max(h_{c,table}; h_{c,CDA})$	
		Table (U_vert) [52]	ΔT [K] $h_{c,table}$ [W/m2K] −1020 0.58 0 0.58 0.5 1.63 2 2.44 7 3.60 30 5.70 50 6.40 1020 10
		CDA – Ceiling Diffuser Algorithm [46]	$h_{c,CDA} = 1.208*\text{red} + 1.012 * \max(0.0, ACH)^{0.604}$ $red = min(5.0, ACH)/5.0$ red – reduction in case of ACH<5
IDA ICE VW	Ventilated window model	$h_c = \max(h_{c,forced}; h_{c,nat})$	
		DNCA - Detailed Natural Convection Algorithm [46]	$h_{c,nat} = \frac{1,81*\lvert\Delta T\rvert^{1/3}}{1,382}$
		VDI Heat Atlas [53]	$h_{c,forced} = Nu*\frac{\lambda}{H}$ $Nu_l = 0.664*\sqrt{Re}*Pr^{\frac{1}{3}}$ $Nu_t = \frac{0.037*Re^{0.8}*Pr}{1+2.443*Re^{-0.1}*\left(Pr^{\frac{2}{3}}-1\right)}$
IES VE	Alamdari & Hammond	[48]	$h_c = \left(\left(1.5\left(\frac{\lvert\Delta T\rvert}{H}\right)^{\frac{1}{4}}\right)^6 + \left(1.23\lvert\Delta T\rvert^{\frac{1}{3}}\right)^6\right)^{\frac{1}{6}}$
TRNSYS	Internal Calculation Method	[33]	$h_c = 1.5*(\Delta T)^{0.25}$
TRNSYS CFS	Complex Fenestration System (CFS)	ISO 15099 [50]	$h_c = 2h_{c,\ enclosed\ gap} + 4v$

experimental monitoring system, wind data was not recorded; hence the effect of the wind condition on the performance of the DSF is not accounted for. However, due to the location of the measurement site and its surroundings, and the type of tested DSF (which does not exchange air mass with the outdoor environment), it is possible to assess that the impact of such missing information is negligible compared to other aspects in the numerical modelling procedure.

2.4. Simulation runs and output processing

The experimental data were used to construct customised weather data files (according to the formats required by the different simulation environments) for the periods to be simulated. The measurements available to create the customised weather data files included the global solar irradiance data on the horizontal plane and the outdoor air temperature. The required weather data are, in addition to the outdoor dry bulb temperature, the direct beam and diffuse horizontal solar irradiance, the cloud cover fraction of the sky, and horizontal infrared radiation intensity from the sky. These quantities related to the solar and infra-red radiative heat exchange have been numerically derived for each time step (hourly) from the experimental data available using the following correlations: Reindl et al. [56] and Perez et al. [57] for the calculation of the beam and diffuse component of the solar radiation; Kasten et al. [58] for the cloudiness factor and Martin et al. [59] for the sky temperature used in the calculation of the infrared radiation from the sky. Sensitivity analysis has been carried out to verify that the uncertainty in the decomposition of the solar irradiance in the direct and diffuse components (which were not directly measured) has little impact on the validation process results. Furthermore, since the measurement of the global irradiance on the vertical (façade) plane was available from the experimental dataset, the goodness of the decomposition procedure adopted was verified by comparing the numerically calculated global solar irradiance on the vertical (façade) plane with the measured value for the same quantity.

The measured indoor air temperature and the test cell's opaque surfaces temperatures were adopted in the simulation to assure identical boundary conditions in all the tools and identical to the experiments. This equivalency was achieved by giving each surface, and the indoor air node (measured) temperature values through schedules created using the available experimental data. This strategy allowed us to replicate the entire set of indoor and outdoor boundary conditions surrounding the DSF. In this way, the validation procedure can focus on the DSF models' performance only because all the other possible uncertainties linked to the different processes in the simulation tools linked to the environments surrounding the DSF were eliminated.

In each tool, the simulation time-step was set to 10 min, and then the numerical outputs were extracted, with a time-step of 1 h, so that the following (simulated) physical quantities could be obtained (See Appendix A, Fig. A.1 and Fig. A.2):

- the (average) air temperature of the cavity [°C];
- the (average) surface temperature of the interior surface of the interior glazing [°C];
- the (average) specific heat flux (i.e. the sum of the convective heat flux exchanged between the surface of the inner skin and the indoor air and the radiative heat flux in the longwave infrared region exchanged between the surface of the inner skin and the surfaces of the room behind the DSF) [W/m^2];
- the transmitted solar irradiance through the entire DSF structure, measured on the vertical plane [W/m^2].

More in details, depending on the exact modelling approach

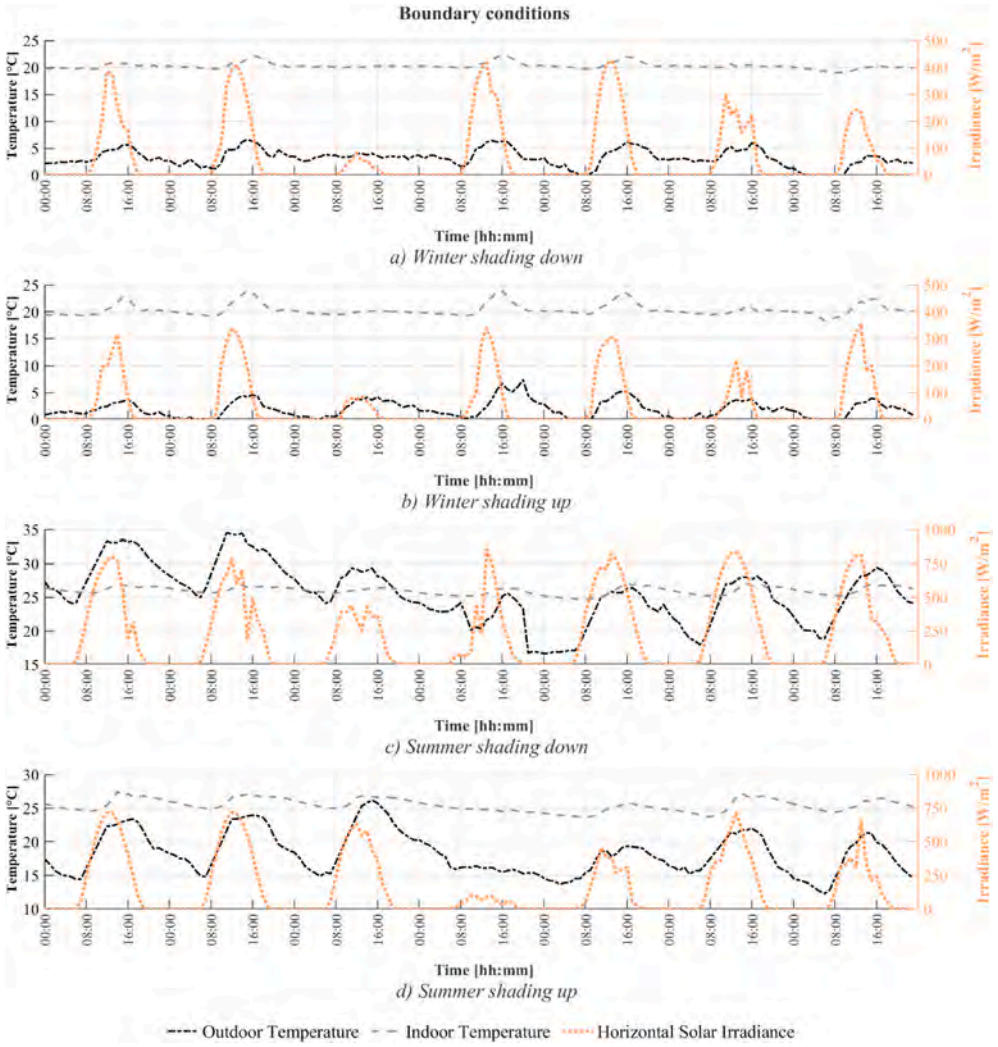

Fig. 4. Time profile of the outdoor and indoor air temperature [°C] and horizontal global solar irradiance [W/m^2] for the four modelling periods: a) Winter with shading down, b) Winter with shading up, c) Summer with shading down and d) Summer with shading up.

adopted, more values for the temperature, the heat flux, and the transmitted irradiance can be obtained – this is typical, for example, for the models with stacked zones, while in the case of models with an in-built component, only one value per façade element is calculated. In order to obtain homogenous information regardless of the adopted modelling approach, area-weighted averages were calculated when more than one value for the same physical quantities was obtained from the simulation.

Furthermore, not all the BES tools allow one to obtain the entire set of quantities used in this validation study: IES VE does not provide the heat flux exchanged by the inner skin with the indoor environment. In some other cases, not all the desired variables are directly available among the output from the software: in the zonal approach in EnergyPlus and TRNSYS, the transmitted solar irradiance can only be obtained by combining different outputs; in the "*Airflow Window*" of EnergyPlus, it is not possible to directly obtain the temperature of the air in the ventilated cavity. In all the cases where the desired quantities could only be derived through intermediate calculations or combinations of different outputs, dedicated data postprocessing was carried out to obtain these parameters.

2.5. Validation procedure

The validation of the different software tools was carried out through combined qualitative and quantitative analyses. This approach provides the possibility to quantify the performance and deepen the understanding of the different observed behaviours. Time profiles of the thermophysical quantities identified in the previous section were useful to support the qualitative (and explanatory) assessment in combination with scatter-plot and error distribution box-plot representations. The quantification of the mismatch between the experimental data and the numerical data was assessed through the calculation of two commonly used statistical indicators, as described in the following equations: the Root Mean Square Error (RMSE) (Eq. (1)) and the Mean Bias Error MBE) (Eq. (3)). The normalised values of these indicators were calculated for evaluating the fitness of the models in predicting the total energy crossing the DSF in one week: Coefficient of Variation of the Root Mean Square Error [CV(RMSE)] (Eq. (2)) and the Normalised Mean Bias Error (NMBE) (Eq. (4)).

$$RMSE = \sqrt{\frac{\sum_{i=1}^{n}(P_i - M_i)^2}{n}} \quad \text{Eq. 1}$$

$$CV(RMSE) = \frac{RMSE}{\bar{y}} * 100 \quad \text{Eq. 2}$$

$$MBE = \frac{\sum_{i=1}^{n}(P_i - M_i)}{n} \quad \text{Eq. 3}$$

$$NMBE = \frac{MBE}{\bar{y}} * 100 \quad \text{Eq. 4}$$

where.

P_i – predicted value by the simulation; Mi – measured value at one point; n – total number of measurements;

$\bar{y}$ – mean value of the measured values.

The RSME indicator quantifies how much the simulated data series differs from other experimental data series by returning the average mean deviation (error) and the degree of data variation. However, this indicator does not provide the error information on whether the mis-prediction underestimates or overestimates the experimental data. The MBE, instead, returns the average bias in the prediction of the simulated data. The MBE should not be used as a measure of the model error since high individual errors in the prediction can still lead to a low MBE value, but since the MBE value has a sign, it can be used to assess whether the overall prediction over-or under-estimates the experimental data. These indicators' normalised values facilitate comparing the tools' performance between the four periods when it comes to the total energy crossing the façade in one week. The NMBE measures how closely the energy use predicted by the model corresponds to the experimental data. CV(RMSE) allows one to determine how well a model fits the data; the lower the CV(RMSE), the better the simulated data. NMBE and CV (RMSE) are performance metrics adopted, among other functions, to assess the match between a calibrated model and experimental data (e.g. ASHRAE Guideline 14 [60]).

3. Results

3.1. Zonal approach versus component modelling

In the first part of the presentation of the results, for each software tool that implements a dedicated in-build model for DSFs, we compared the performance of such a dedicated routine and the zonal modelling approach. This is done for EnergyPlus, IDA ICE and Trnsys. For each of these tools, only the best performance approach is later compared with the other tools in Section 3.2.

3.3.1. Energy Plus

The comparison between the simulations carried out with the zonal approach and the Airflow Window model is shown below in Fig. 5 (as previously described, all the values for the given physical quantity in the stacked multi-zone model have been averaged to one single value for each variable). The scatter plots show the results of all the four analysed periods combined.

Among the two models, the zonal approach shows the worse fit to the experimental data for all the different parameters selected for the validation procedure (Table 5). The two models show different behaviour in predicting the air gap temperature; this behaviour also depends on the shading device's presence in the cavity. Compared to observations (see results of the zonal model in Fig. 5), the zonal approach overestimates the air temperature in the ventilated cavity, especially in the upper range at high airgap and surface temperatures, and over a wide range of heat flux values. The Airflow window model highly underestimates the peaks when the shading system is inside the cavity (Fig. 6a and c), while the zonal model has relatively good results while still underestimating the predictions.

Conversely, when the shading system is not deployed (i.e. rolled up), the zonal model highly overestimates the air gap temperature (Fig. 6b and d). The time distribution of the surface temperature and the heat flux shows that the two models have good predictions, and they are more or less equivalent when the shading system inside the cavity is activated. For both models and seasons, the RMSE value of the heat flux is around 10 W/m^2. This behaviour changes dramatically when the shade is not used: the errors in the predictions of the heat flux of the zonal approach reach up to four times the measurement data ($RMSE_{Winter,\ ShOFF} = 40$ W/m^2, $RMSE_{Summer,\ ShOFF} = 32$ W/m^2).

Moreover, the EnergyPlus' zonal approach leads to a great under-prediction of the solar irradiance transmitted to the room behind the DSF. The algorithm implemented for the processing of diffuse irradiance through thermal zones in this tool distributes the diffuse incoming irradiance evenly on all the surfaces of the thermal zone [23]. In the zonal approach, the ventilated cavity is modelled as a series of thermal zones, and therefore, the diffuse component of the solar irradiance

Table 5
MBE and RMSE values calculated for the two EnergyPlus models.

	EnergyPlus Zone Model		EnergyPlus Airflow Window	
	MBE	RMSE	MBE	RMSE
Air gap temperature [°C]	0.9	4.5	−0.9	3.9
Surface temperature [°C]	0.6	3.1	−0.2	2.4
Heat flux [W/m^2]	7.5	27	0.2	14
Solar irradiance [W/m^2]	−7.9	22	0.9	13

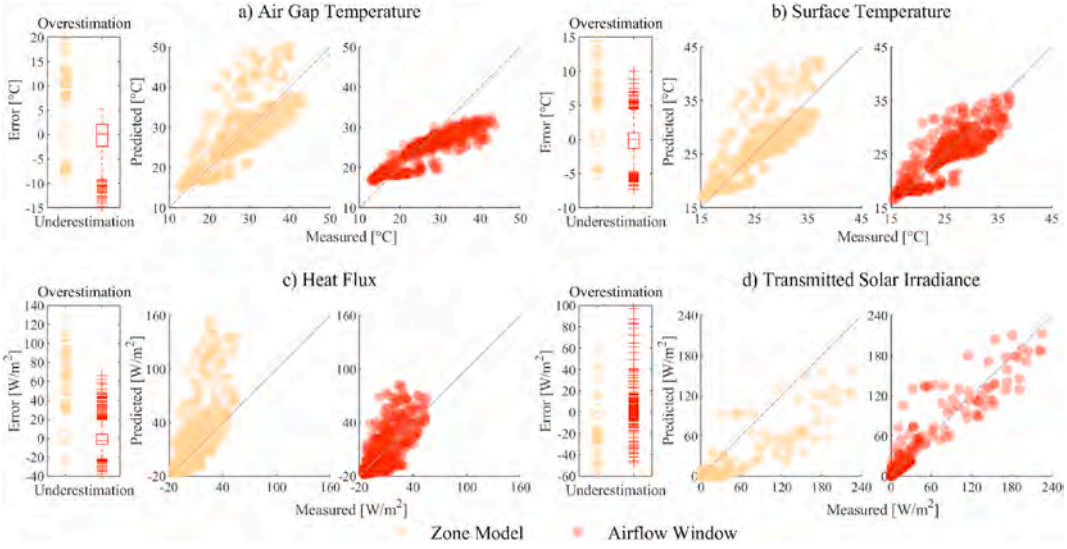

Fig. 5. Comparison between predicted and experimental data for the two models carried out in Energy Plus. a) Air Gap Temperature b) Inner glass surface temperature c) Heat flux d) Transmitted solar irradiance. The four simulated periods are combined.

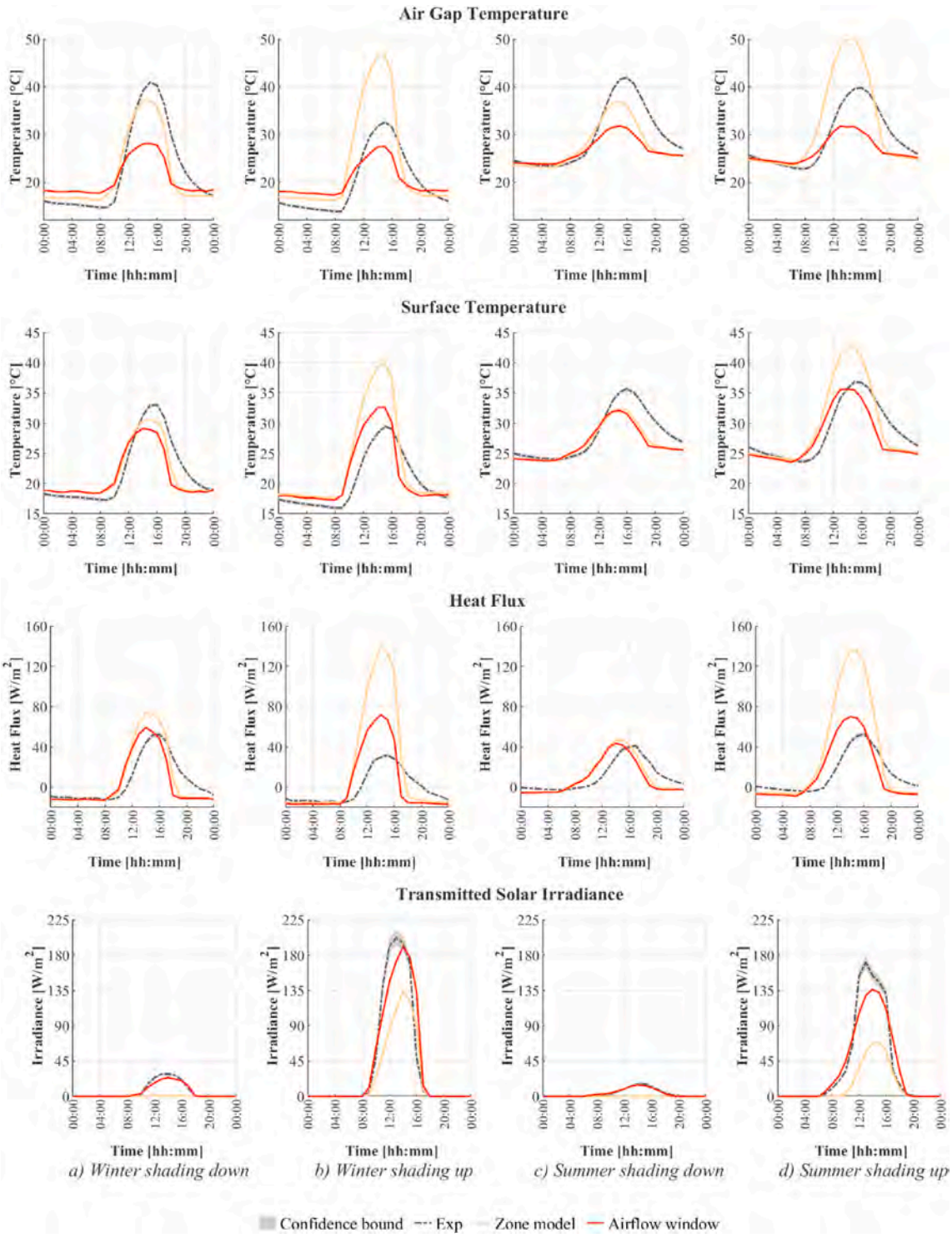

Fig. 6. Time distributions of the two Energy Plus models predictions in the four configurations. Air gap temperature. Surface temperature. Heat flux. Transmitted solar irradiance. a) Winter shading down, b)Winter shading up, c) Summer shading down, d) Summer shading up. A single, representative day was selected from the simulated periods.

transmitted through the external skin of the DSF is evenly distributed on all the surfaces that delimit the ventilated cavity – hence the outer skin, the inner skin, the virtual surfaces at the top and bottom of each volume in which the cavity is divided, and the sides of the cavity. When the roller screen is deployed, because of EnergyPlus treating the shade as a perfect diffuser, the total irradiance transmitted through the shading (both the direct and the diffuse component) is considered diffuse and thus evenly distributed on every surface of the thermal zone. These procedures lead to the fact that the solar irradiance is not treated correctly when this modelling approach is adopted, and a substantial underestimation of the direct solar gain in the room behind the DSF is revealed.

In light of these results, it was chosen to use the 'Airflow Window' model to continue with the other software comparison.

3.1.2. IDA ICE

The comparison between the performances of the two models of IDA ICE is shown in Fig. 7, where we adopted the same procedure as for the illustrations related to EnergyPlus (i.e. the results of the zonal model have been averaged to one single value, and the charts include the results of all the four analysed periods).

The two models give quite similar results for all the evaluated parameters. The ventilated window model shows a slightly better fit in replicating the heat flux and the transmitted solar irradiance while showing a slightly worse fit in predicting the air gap temperature. As shown in Table 6, the two models predict the surface temperature of the inner glazing with the same accuracy.

Observing the time profiles (Fig. 8), it is possible to notice that the models' predictions changes if the shades are present in the cavity or not. It appears that the prediction of the air gap temperature is more accurate if the shading is not activated (with a better prediction of the ventilated window model in winter – $RMSE_{Winter,\ ShOFF} = 1.5\ °C$ (Fig. 8 b) and a better prediction of the zonal approach in summer – $RMSE_{Summer,\ ShOFF} = 1.4\ °C$ (Fig. 8 Time distributions of the two IDA ICE models predictions in the four configurations. Air gap temperature. Surface temperature. Heat flux. Transmitted solar irradiance. a) Winter shading down, b)Winter shading up, c) Summer shading down, d) Summer shading up. A single, representative day was selected from the simulated periods. d)). When the shading system is on (Fig. 8 a and c) both models underpredict the results. Similar behaviour is seen for the surface temperature, except that both models predict this variable very well during the summer without the shading in the cavity (Fig. 8 d)).

The heat flux exchanged at the indoor interface of the DSF is overpredicted by both models, especially when the shades are rolled up (off); during summer, the predicted peaks are more than three times higher compared to the measured ones ($RMSE_{Summer,\ ShOFF} = 22\ W/m^2$ for the zonal model and 20 W/m^2 for the inbuilt model - Fig. 8 d)). Instead, the two models underpredict the transmitted solar irradiance during the same periods. There is also a significant difference between the two predictions, which is most likely due to the zonal approach's modelling limitations, where the horizontal partitions need to be opaque components, and thus, this feature may impact the overall optical losses within the system.

Because the 'Ventilated window' model offers slightly better results, and to make use of such an in-built model in IDA ICE is faster than implementing a model based on the zonal strategy, this approach has been chosen for the multi-tool comparison that follows in the next section.

Table 6
MBE and RMSE values calculated for the two IDA ICE models.

	IDA ICE Zone Model		IDA ICE Ventilated Window	
	MBE	RMSE	MBE	RMSE
Air gap temperature [°C]	−0.1	2.5	−0.3	2.6
Surface temperature [°C]	0	1.6	0.4	1.5
Heat flux [W/m^2]	3.5	17	2.6	15
Solar irradiance [W/m^2]	−3.7	22	0.2	21

3.1.3. TRNSYS

The comparison between the performances of the two models of Trnsys is shown in Fig. 9, where we adopted the same procedure as for the illustrations related to EnergyPlus and IDA ICE (i.e. the results of the zonal model have been averaged to one single value, and the charts include the results of all the four analysed periods). The module for implementing a 'Complex Fenestration System – CFS' is only available in a version of Trnsys18 released in 2020, while the zonal approach was implemented in a prior version of this tool (Trnsys17), which can be also used in the newer version Trnsys18.

Among the two models, the zonal approach shows a better fit to the experimental data for most of the parameters selected for the validation procedure (Table 7). The two models show similar behaviour in predicting the air gap temperature when the shading device is not in the cavity. Compared to observations (see the zonal model results in Fig. 9), the zonal approach underestimates the air temperature in the ventilated cavity, especially in the upper range at high airgap and surface temperatures. Conversely, the CFS model shows an overestimation over a wide range of heat flux values and solar irradiance.

When observing the time profiles (Fig. 10), it is possible to notice that the models' predictions change if the shades are present in the cavity or not. It appears that the prediction of the air gap temperature is more accurate if the shading is not activated, with a very similar prediction of the peaks from both models in winter and summer (Fig. 10 b and d). Nevertheless, the statistical values show a better agreement of the zonal approach to the experimental data ($RMSE_{Winter,\ ShOFF,\ Zonal} = 2.8\ °C$ *vs.* $RMSE_{Winter,\ ShOFF,CFS} = 3.5\ °C$ and $RMSE_{Summer,\ ShOFF,\ Zonal} = 2.6\ °C$ *vs.* $RMSE_{Summer,\ ShOFF,CFS} = 2.8\ °C$). When the shading system is on (Fig. 10 a and c) both models underpredict the results. Different behaviour is shown in the surface temperature: both models

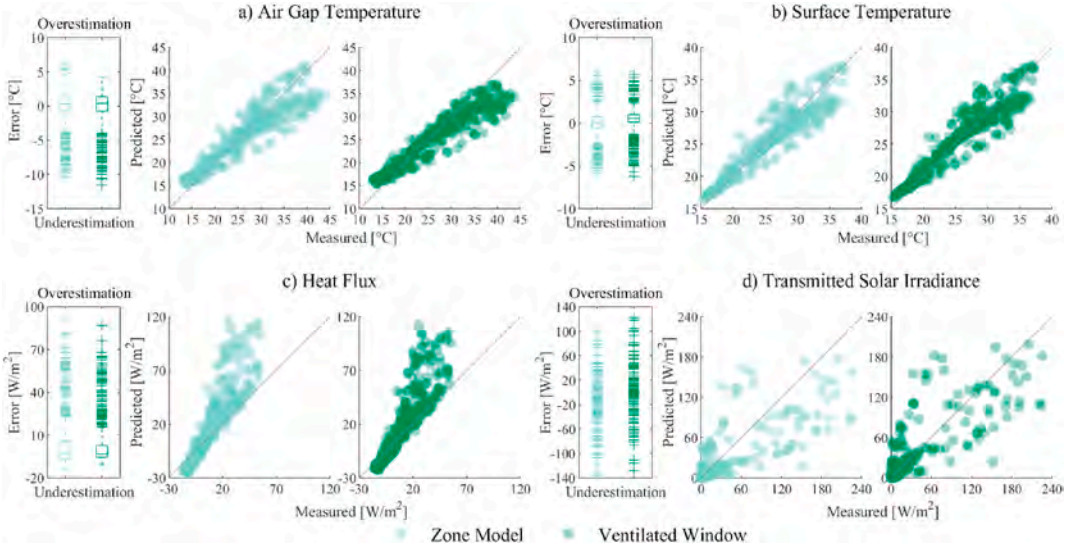

Fig. 7. Comparison between predicted and experimental data for the two models carried out in IDA ICE. a) Air Gap Temperature b) Inner glass surface temperature c) Heat flux d) Transmitted solar irradiance. The four simulated periods are combined.

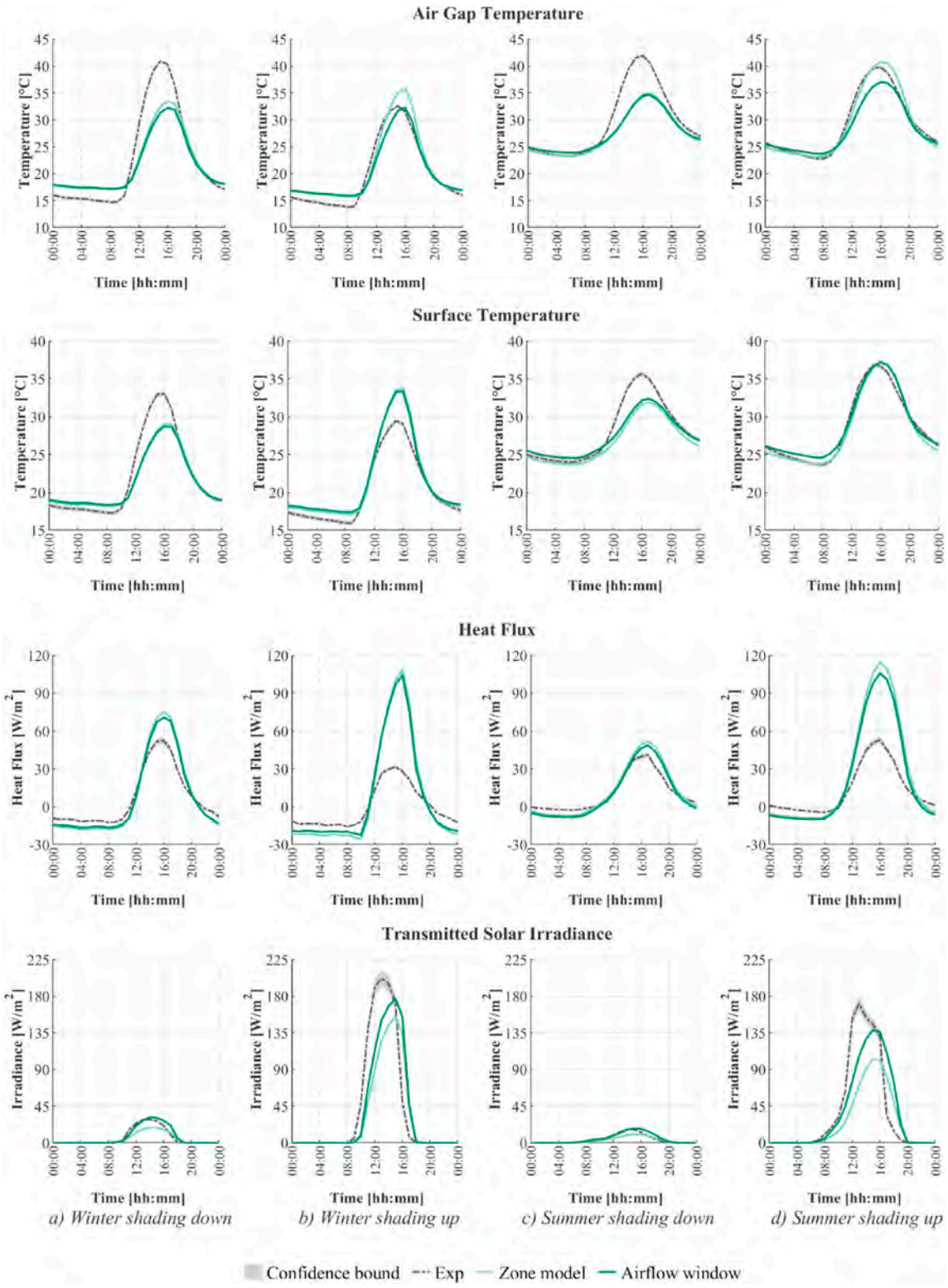

Fig. 8. Time distributions of the two IDA ICE models predictions in the four configurations. Air gap temperature. Surface temperature. Heat flux. Transmitted solar irradiance. a) Winter shading down, b)Winter shading up, c) Summer shading down, d) Summer shading up. A single, representative day was selected from the simulated periods.

underpredict this variable with the shading in the cavity (Fig. 10 a and c), the zonal model offers a better prediction in winter without the shading device ($RMSE_{Winter,\ ShOFF} = 1.8$ °C - Fig. 10 b) while the CFS model performs better in summer ($RMSE_{Summer,\ ShOFF} = 2$ °C - Fig. 10 d).

The heat flux exchanged at the indoor interface of the DSF is overpredicted by both models at night in all four periods. When the shades are rolled up (off), the CFS model's predicted peaks are highly overpredicted. The zonal approach performs better in summer than in winter ($RMSE_{Summer,\ ShOFF} = 11$ W/m^2 $RMSE_{Winter,\ ShOFF} = 13$ W/m^2 - Fig. 10 b and d). There is a significant difference in predicting the

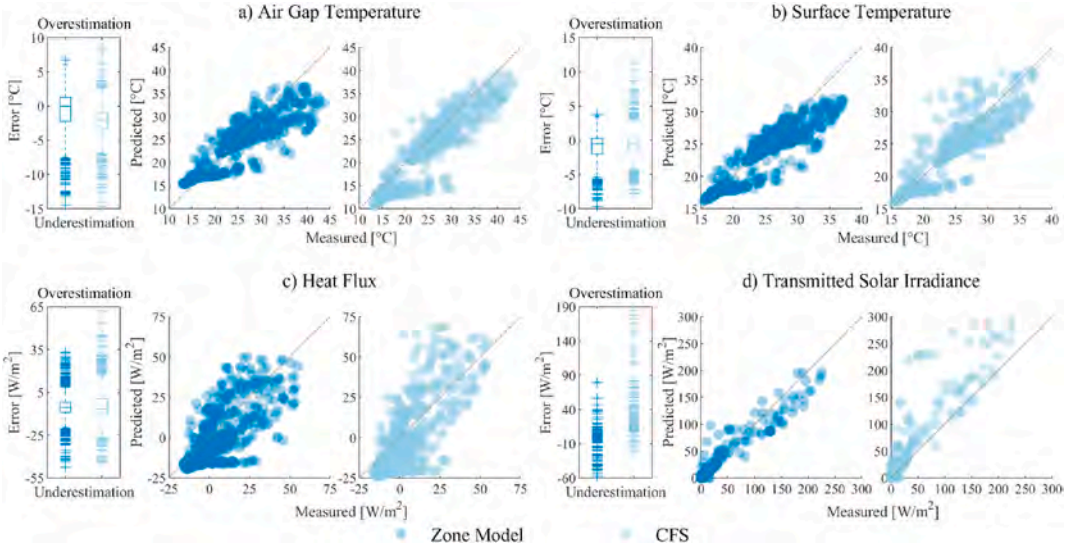

Fig. 9. Comparison between predicted and experimental data for the two models carried out in Trnsys. a) Air Gap Temperature b) Inner glass surface temperature c) Heat flux d) Transmitted solar irradiance. The four simulated periods are combined.

Table 7
MBE and RMSE values calculated for the two Trnsys models.

	Trnsys Zone Model		Trnsys CFS model	
	MBE	RMSE	MBE	RMSE
Air gap temperature [°C]	−0.9	3.5	−2.3	3.7
Surface temperature [°C]	−1.1	2.4	−0.6	2.5
Heat flux [W/m^2]	−4.9	12	−3.8	14
Solar irradiance [W/m^2]	−1	10	7.5	25

transmitted solar irradiance between the models; the CFS model overpredicts the results while the zonal approach underpredicts them. This behaviour is more accentuated in the winter periods. This difference is most likely connected to the changes made to the solar radiation routines in version 18 of Trnsys, and the model adopted to decompose the global solar radiation [61]: the zonal model was implemented in Trnsys17 while the CFS model is only available in the last release of Trnsys18.

Because the 'Complex Fenestration System' model does not offer significantly better results, and to make use of such an in-built model in Trnsys, BDSF data for the glazing and the shading device are needed making it more complicated than implementing a model based on the zonal strategy, this approach was not chosen for the multi-tool comparison. Moreover, one of the model's features is that it is impossible to connect the indoor zone's temperature node to the inlet of the façade since the inlet's temperature has to be set (or fixed or a schedule). This limits the applicability to a real case, where the inlet temperature is not known, or the indoor temperature does not correspond to the set input of the HVAC system. Thus, the zonal approach model will be used in the next section.

3.2. Intersoftware comparison for thermophysical quantities

This section gives an overview of the four analysed tools' overall performance for the chosen physical quantities. As previously described, for the tools providing an in-built model of DSF, the in-built model approach has been generally selected to perform the comprehensive comparison with all the BES tools, as these showed slightly more reliable results. When, due to different reasons, the comparison has been carried out using, for each tool, the results from the zonal modelling approach, this is specified in the text.

3.2.1. Air gap temperature

Fig. 11 shows the errors in predicting each model's air gap temperature in the four BES tools. IDA ICE is the software that returns the most accurate prediction of this variable when all the four periods used in the validation procedure are considered together. Similarly, the magnitude of Energy Plus, Trnsys and IES-VE error is similar. In general, the tools underestimate the temperature during the day and overestimate the lower values, particularly during the winter nights. Particularly, Energy Plus performs poorly, significantly underestimating the peaks all the time.

In general, it is possible to say that all the tools underpredict the intensity of the peaks (Fig. 12). The prediction of EnergyPlus, Trnsys and IES VE is very similar when the shadings are deployed (Fig. 12 a and c): all of them highly underpredict the peaks during the day. IDA ICE performs slightly better than the tools mentioned above whilst still underpredicting the values to a great extent. IDA ICE tends to underestimate the peaks except during the winter period when there is no shading device in the cavity ($RMSE_{Winter,\ ShOFF}$ = 1.5 °C - Fig. 12 b). In this period, Trnsys gives very similar results to IES VE, slightly underpredicting the peaks, while EnergyPlus is the worst performing tool. In the summer case where the shading is not in the cavity (Fig. 12 c), Trnsys, IDA ICE and IES VE give almost the same prediction of the peaks. EnergyPlus, as previously said, is the worst-performing software tool by always underpredicting the temperature in the warmest hours of the day.

We can see a tendency in IDA ICE of a small delay in predicting the peaks compared to the experiments and of one to 2 h compared to the other tools. When it comes to Energy Plus, TRNSYS, and IES-VE, these tools anticipate the peak values compared to the experimental data. These time shifts become even more evident in predicting the surface temperature and heat flux. We can assume that they are due to a series of modelling simplifications in some simulation environments (lack of the glazing capacity node in all tools except IDA ICE), the processing of solar irradiance and other input variables related to the outdoor environment (e.g. how the solar irradiance is decomposed from the hourly weather data file in intermediate, sub-hourly values), and how simulation results with sub-hourly time-steps are post-processed to obtain hourly values.

The four tools produce all consistently high errors in predicting the air temperature at night-time during the winter season, while this effect is not as evident during the summer. The inability to reproduce air gap temperatures as low as the observations at night may come from the different inlet temperature used in the model (which corresponds to the

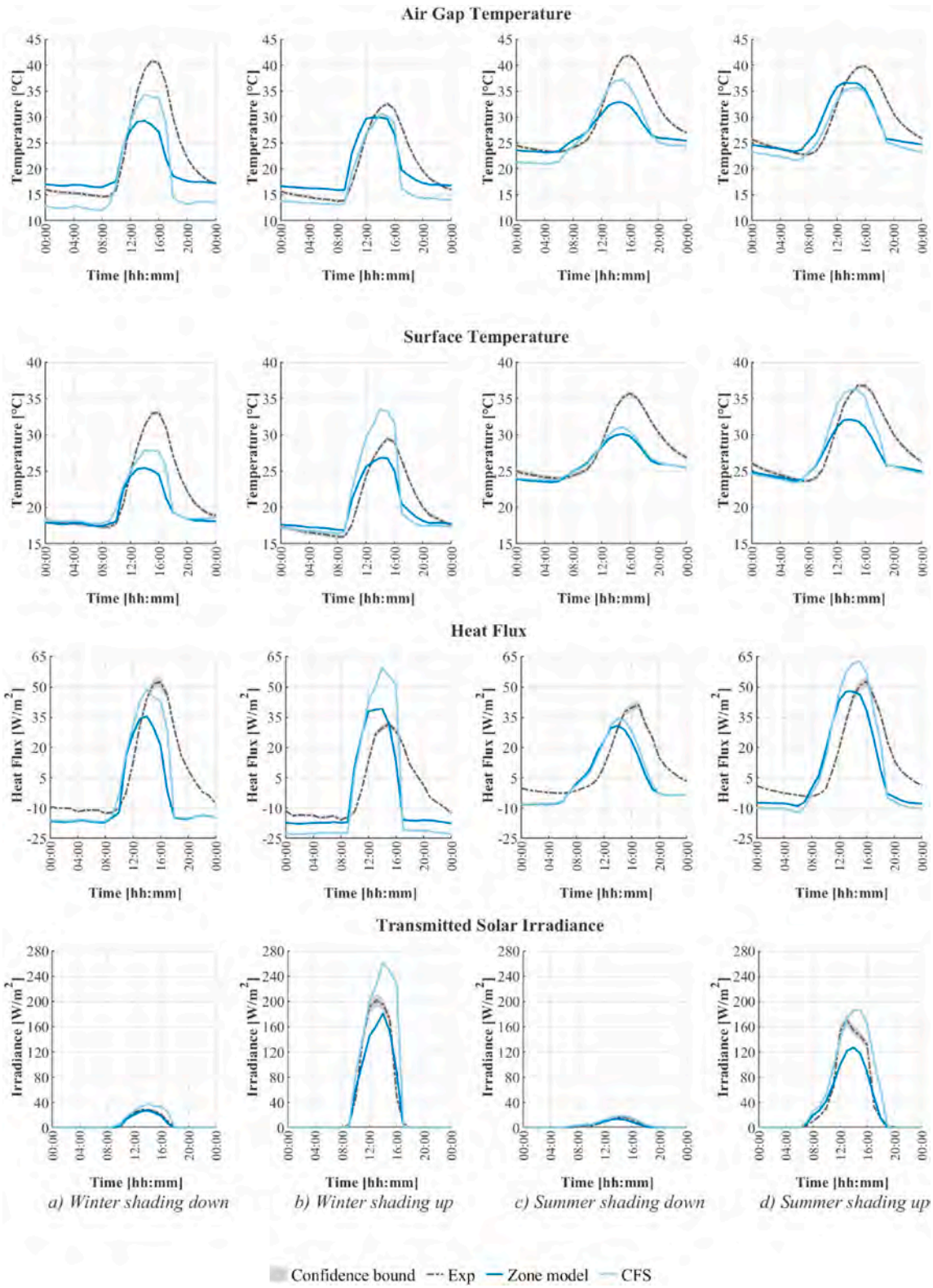

Fig. 10. Time distributions of the two Trnsys models predictions in the four configurations. Air gap temperature. Surface temperature. Heat flux. Transmitted solar irradiance. a) Winter shading down, b)Winter shading up, c) Summer shading down, d) Summer shading up. A single, representative day was selected from the simulated periods.

indoor air temperature) and the experiments' actual conditions. We hypothesise that, as the air enters the DSF's cavity after crossing the aluminium frame at the bottom of the DSF, the airflow undergoes some heat loss due to the heat exchange with the bottom cavity surface. This effect can be visualised by looking at the detailed results obtained from each stacked zone in the simulations using the zonal approach (Fig. 13). Only for this specific comparison, the results of the zonal approach of all the tools are used (instead of the in-built models of Energy Plus and IDA

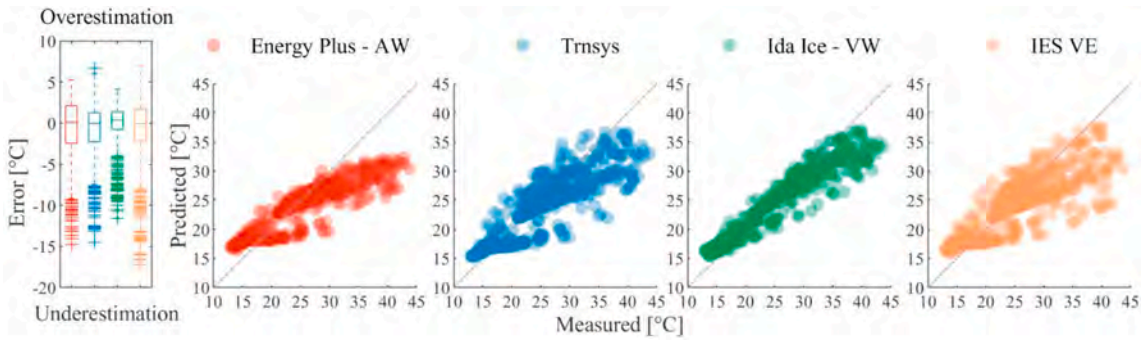

Fig. 11. Comparison between measured data and predicted air gap temperature values. The four simulated periods are combined.

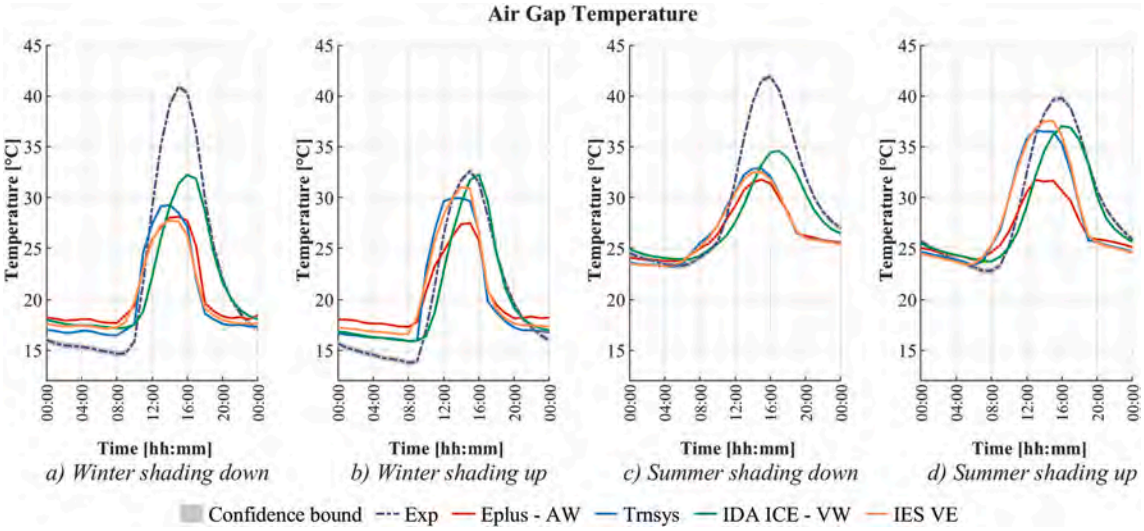

Fig. 12. Time profiles of the air gap temperature prediction in the four configurations. A single, representative day was selected from the simulated periods.

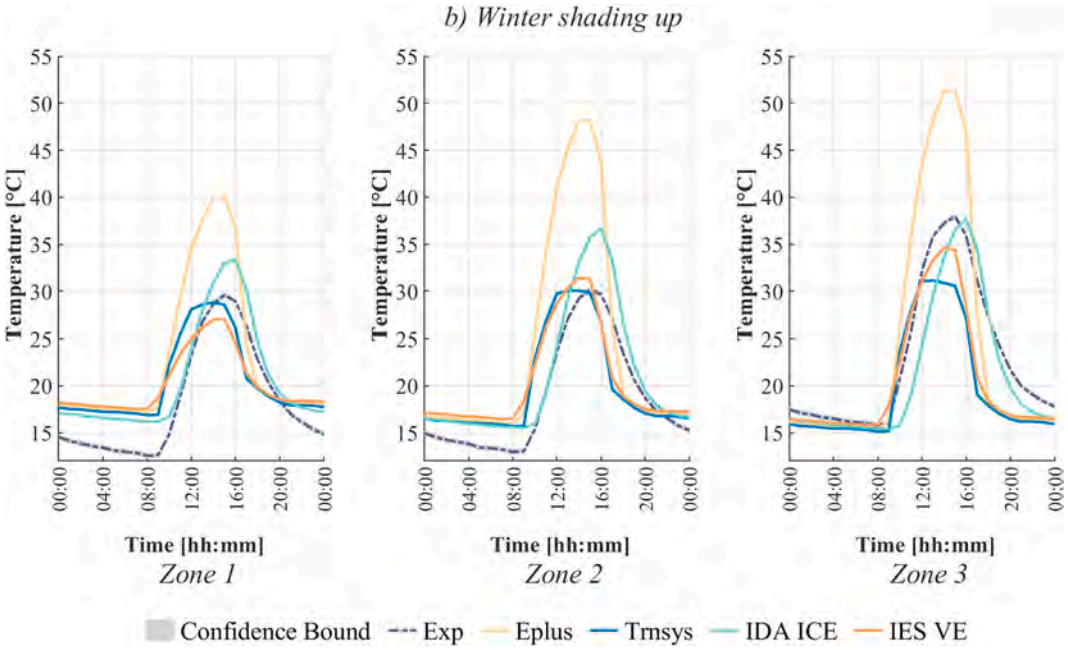

Fig. 13. Time profiles of the vertical distribution of the air gap temperature. Winter period with the shading in the cavity. The graph shows the results of the model with the zonal approach of Energy Plus and IDA ICE.

ICE). The vertical temperature profile shows different errors in the daytime and the night-time. In all the tools, the first (lowest) thermal zone has the lowest temperature, and the cavity air temperature rises with the zone's vertical position. At night time, the temperature values are similar in all tools with an overprediction of the air gap temperature in the first thermal zone, while the predicted temperatures in the third thermal zone overlap the measurements. During the daytime, the results of the tools show a higher spread. The results show a moderate vertical temperature rise in TRNSYS and IDA ICE: the former shows a good agreement with the experiments in the lower two zones, the latter in the third zone. Energy Plus results show a high overprediction of the peaks in all the three zones, while IES VE shows differences of moderate intensity, with the overprediction of the air gap temperature seen only in the middle zone – an effect that is difficult to find an explanation for.

3.2.2. Surface temperature (of the inner skin)

IDA ICE is the best performing tool (Fig. 14) in predicting the surface temperature, as quantified by the statistical indicators and observed in the scatter plot graphs, which consider all four periods together. Conversely, by observing the time profile distribution, it is possible to notice that IDA ICE predicts the peaks significantly more correctly than the other tools in only one period (summer, shading not deployed) out of four ($RMSE_{Summer,\ ShOFF} = 1\ ^{\circ}C$ Fig. 15 d). During the other periods, the peak prediction is very much in line with the results of EnergyPlus. As in predicting the air gap temperature, EnergyPlus, TRNSYS, and IES VE predict the values one or 2 h ahead of the measurement and IDA ICE's predictions. This latter discrepancy is not highlighted in the statistical indicator, so even if IDA ICE has a more significant error in terms of magnitude, it appears to be the one with better performance in predicting this quantity. As previously explained, we believe that this effect can be to a great extent explained by the fact that IDA ICE implements a capacitive node in the glass calculation model – a feature that is missing in the other three BES tools.

It is impossible to define a clear and robust trend on how the tools perform depending on the season, as the overestimation and underestimation are seen within the same period. In general, the time profiles and values have the smallest errors in summer without the shading in the cavity (Fig. 15 d). All the tools tend to underpredict the peak values with shading on, both summer and winter, and overpredict night time values in winter (with the only exception being TRNSYS). In winter, without the shading deployed, almost all the tools (except for Trnsys) overestimate the peaks (Fig. 15 b).

3.2.3. Heat flux (exchanged at the indoor-facing interface of the inner skin)

As it is not possible to extract this information from IES VE, the comparison of the heat flux values' prediction is carried out for the three other tools. The general trend is an overprediction of the peaks and an underestimation of the lower values by EnergyPlus and IDA ICE, and a more accurate prediction by TRNSYS (Fig. 16). In particular, IDA ICE has the highest errors in predicting the high peaks in three of the four periods, while the values show a good match in summer when the shading is activated.

The time distribution charts also show a common trend towards overestimation for EnergyPlus and IDA ICE, with the worse outputs from all the tools with the shading rolled up (not deployed) (Fig. 17 b and d). When the shading system is present in the cavity, TRNSYS underpredicts the peaks. IDA ICE represents quite accurately the peaks in summer when the shading is deployed in the cavity but becomes far less accurate when the shading is retracted. Once again, EnergyPlus and TRNSYS are ahead of the measured data while IDA ICE predicts at the right time, the values of the heat flux exchanged at the indoor-facing surface of the inner skin. The measurement of the heat flux exchanged at the indoor glazing surface is affected by both the sensor's presence and the shielding installed to avoid overheating due to the solar radiation, as explained more in details in Ref. [54]. However, as previously mentioned, the procedure adopted for monitoring the surface heat flux is, to our best knowledge, the best practice for such a measurement that minimises the experimental uncertainty.

3.2.4. Transmitted solar irradiance

The prediction of the solar irradiance transmitted through the entire double-skin façade, and sampled right at the inner skin's indoor interface is shown in Fig. 18. In this case, EnergyPlus (when the Airflow window model is used) is the software tool that offers the most accurate prediction yet underestimating the high peaks during sunny days (Fig. 19). The tools show similar results when the shading is deployed in the cavity. IES VE tends to overpredict the transmitted solar irradiance values when the shading is not present, while IDA ICE underestimates them. The measurement of the transmitted solar irradiance is also affected by some limitations due to the experimental setting. It includes a component (though almost negligible) of diffuse solar irradiance in the indoor environment which is retro-reflected towards the sensor by the glazing surface, as explained more in details in Ref. [54]. This may result in a measured transmitted irradiance that is slightly higher than the "real" one, though such an error may be considered included in the measurement chain's total accuracy for transmitted solar irradiance.

4. Discussion and possibilities for future developments of BES tools

The time distribution of the predicted values (Figs. 12, Figure 15, Figure 17, Figure 19) shows that there is no single tool that outperforms the others in all the different configurations tested. In most cases, the software representing the daytime peak of a particular physical quantity in winter with the shading down is committing a significant error in predicting another physical quantity in the same period. Therefore, it is not straightforward to rank the tools in an absolute way. We believe it is somehow more appropriate to define the simulation environment that provides the best result for each of the analysed physical quantities. Similarly, it is impossible to say which configuration or period is the

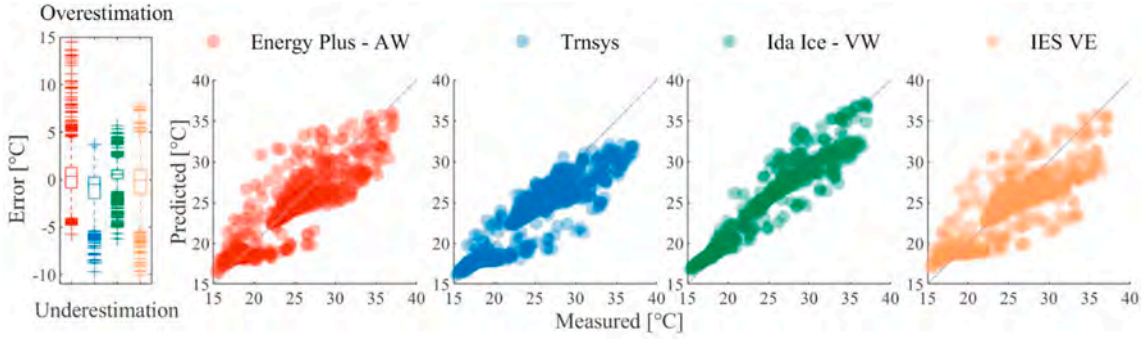

Fig. 14. Comparison between measured data and predicted values of the surface temperature. The four simulated periods are combined.

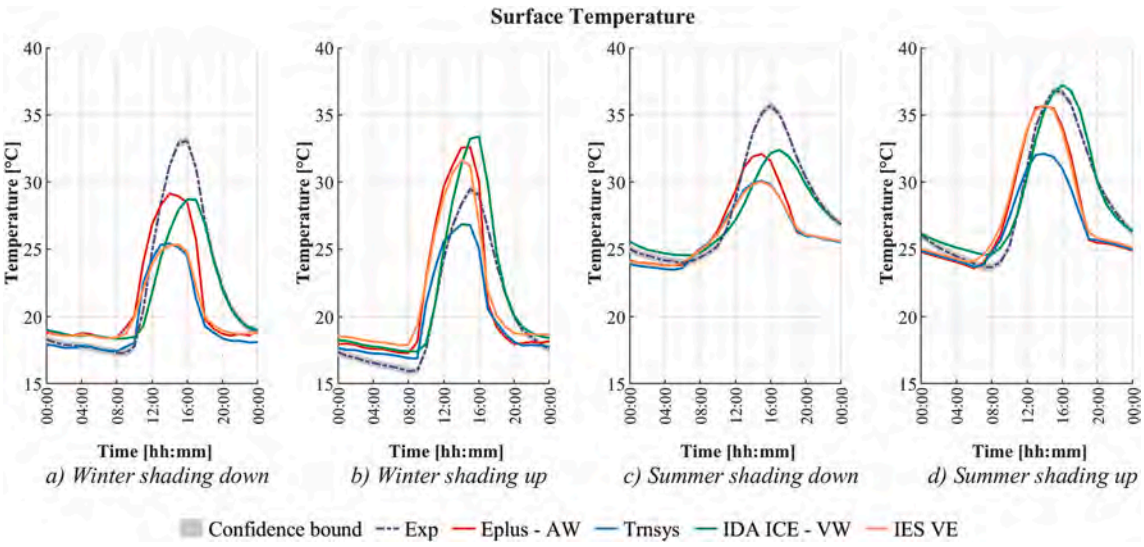

Fig. 15. Time profiles of the surface temperature prediction in the four configurations. A single, representative day was selected from the simulated periods.

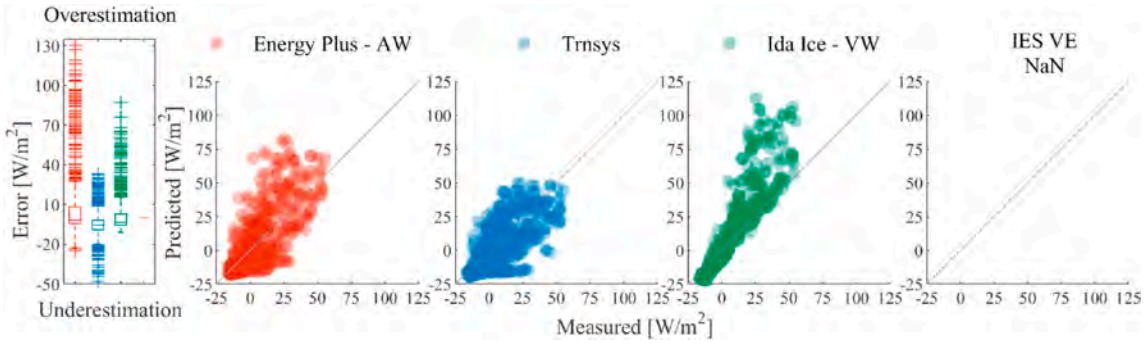

Fig. 16. Comparison between measured data and predicted values of the heat flux. The four simulated periods are combined.

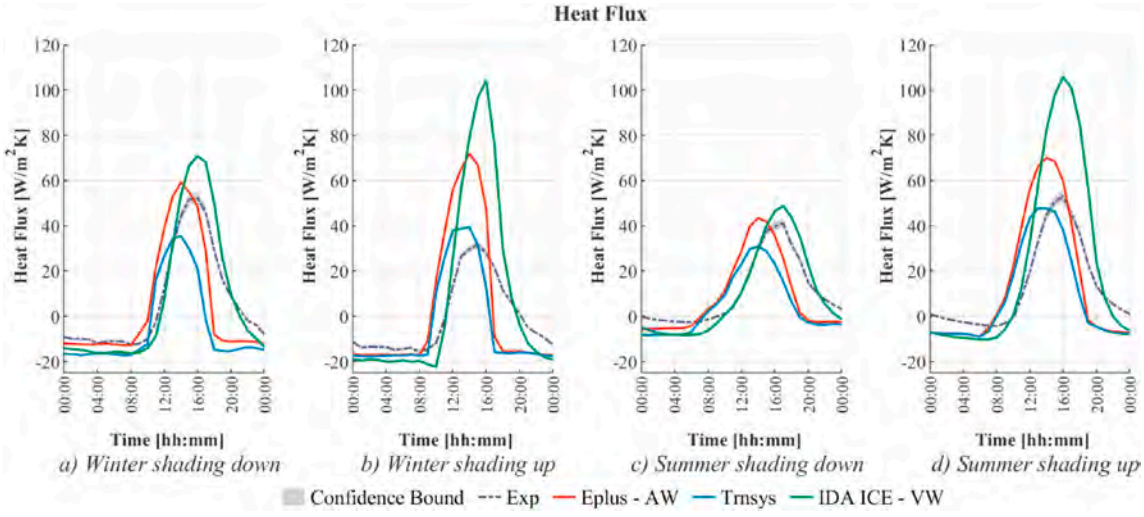

Fig. 17. Time profiles of the heat flux prediction in the four configurations. A single, representative day was selected from the simulated periods.

easiest to be predicted correctly by all the tools.

The statistical indicators for all the analysed physical quantities of the four periods combined are shown in Table 8. According to these values, IDA ICE is the best tool, in terms of fitness of the prediction, when predicting the air gap temperature and the interior glazing surface temperature. EnergyPlus provides the best results for predicting the heat flux and the solar irradiance transmitted through the component. However, these pictures are based on the tools' overall performance, while if the focus is placed on a particular configuration (shading up or down) and a particular season (cold season or warm season), the reliability of the different tools varies to a greater extent.

IDA ICE is very accurate in predicting the surface temperature only

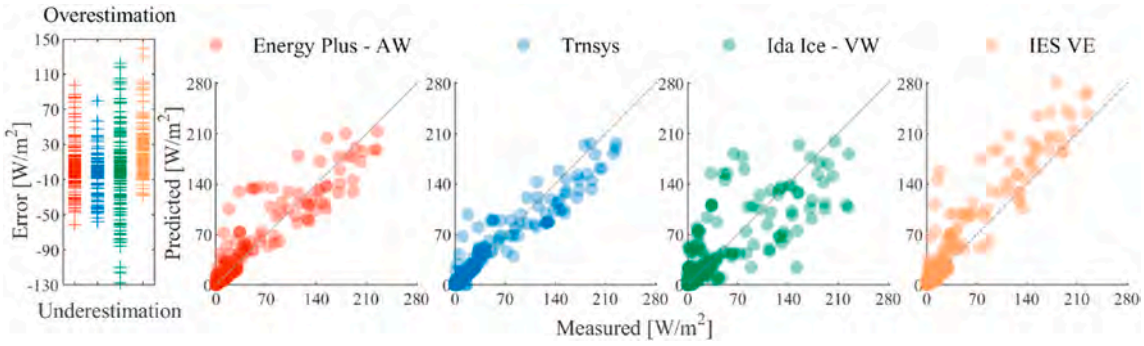

Fig. 18. Comparison between measured data and predicted values of the transmitted solar irradiance.

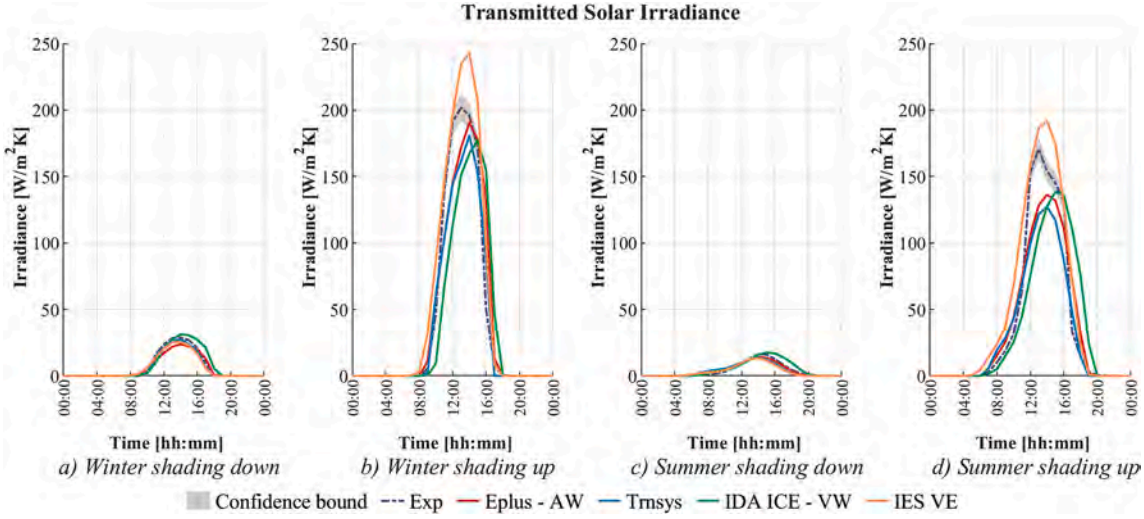

Fig. 19. Time profiles of the transmitted solar irradiance prediction in the four configurations A single, representative day was selected from the simulated periods.

Table 8
MBE and RMSE values calculated for the model in Energy Plus 'Airflow Window', TRNSYS, IDA ICE 'Ventilated Window' and IES<VE>.

	EnergyPlus AW		TRNSYS		IDA ICE VW		IES VE	
	MBE	RMSE	MBE	RMSE	MBE	RMSE	MBE	RMSE
Air gap temperature [°C]	−0.9	3.9	−0.9	3.5	−0.3	2.6	−0.9	3.9
Surface temperature [°C]	−0.2	2.4	−1.1	2.4	0.4	1.5	−0.5	2.6
Heat flux [W/m^2]	0.2	14	−4.9	12	2.6	15	N/A	N/A
Solar irradiance [W/m^2]	0.9	13	−1	10	0.2	21	4.6	17

when the shading is up but commits considerably high errors in the other periods, even if the statistical indicators seem to show a different behaviour. Energy Plus is the worst tool in predicting the air gap and surface temperature but is accurate in predicting the transmitted solar irradiance.

The presence of the shading device in the cavity cannot be identified

Table 9
Performance overview of the tools in the four different periods. Comparison with the experiment results in the two seasons, Winter and Summer, with the shading ON or OFF. - - - Very high underestimation; - - High underestimation; - Underestimation; = Good Agreement; + Overestimation; ++ High Overestimation; +++ Very High Overestimation; N.A. Data Not Available. Colour code: Red: large error; Orange: moderate error; Yellow: small error; Green: accurate prediction.

Tool	***EnergyPlus AW***				***TRNSYS***				***IDA ICE VW***				***IES VE***			
Season	**Winter**		**Summer**		**Winter**		**Summer**		**Winter**		**Summer**		**Winter**		**Summer**	
Shading	**ON**	**OFF**	**ON**	**OFF**	**ON**	**OFF**	**ON**	**OFF**	**ON**	**OFF**	**ON**	**OFF**	**ON**	**OFF**	**ON**	**OFF**
Air gap temperature [°C]	- -	-	- -	-	- -	-	- -	-	- -	+	- -	-	- -	+	- -	-
Surface temperature [°C]	-	+	-	+	-	-	-	-	-	+	-	+	-	+	- -	=
Heat flux [W/m^2]	+	+ + +	=	++	-	+ +	=	+ +	++	+ + +	=	+ + +	*N.A.*	*N.A.*	*N.A.*	*N.A.*
Solar irradiance [W/m^2]	=	- -	=	- -	=	- -	=	- -	=	- -	=	- - -	=	+ + +	=	+ +

as a condition that increases the DSF model's complexity, so that it leads to an increase in inaccuracy and prediction errors. Except for EnergyPlus, all the tools are quite reliable in predicting the air gap temperature when the shading is up, but its presence does not affect the accuracy of the better performing tool (IES VE) in predicting the air gap temperature (Table 9). Conversely, it has a more significant impact on EnergyPlus, TRNSYS and IDA ICE results, where the air gap temperature is highly underpredicted. EnergyPlus and TRNSYS offer an even better prediction of the heat flux when the shading is in the cavity rather than when it is not deployed. However, having the shading device activated leads to an underprediction of the surface temperature by all the tools.

The user can set the simulation's time-step and the output results, but there is no control over how this data is aggregated on an hourly basis. The tools' different approach may lead to a discordance over the final results if dynamic variables are considered. These discrepancies are not visible if daily or periodic data are compared. The use of periodic data is interesting, for example, when the focus is not on the DSF itself but on the influence of installing a DSF has on the energy balance. When comparing the energy gained and lost by the DSF over seven days (Table 10), the performance of the tools is very similar, particularly in those periods when the shading is present in the cavity. All tools tend to over predict the total transmitted energy, but TRNSYS has the overall best performance (Table 11). Using this metric, the tools' behaviour appears to be more in line with the experimental data, and the daily variations seen analysing the dynamic parameters are no longer distinguishable.

In most of the tools, the absence of a capacitive node of the glazing system is reflected in a considerate lagging of the predictions compared to the experimental data. While IDA ICE includes a heat capacity node for the glazing and the shading, the glazing's thermal inertia is not implemented in any of the other models. Hence, any heat absorbed by the glass surface shows an instantaneous effect on the glass temperature, causing a higher temperature rise than in reality. This can have a limited effect when considering a conventional single skin glazing system, usually composed of a total thickness of glass in the range of around 1 cm. In that case, the inertial characteristics of the glazing are relatively low, and the impact of this feature on the dynamics of the heat transfer is somewhat limited – if not negligible. However, when modelling a DSF, the simulated system has a relatively thick glass structure (up to 4–5 cm when considering both skins), and a more precise accounting of the heat absorbed and released because of the specific heat capacity of the material is no longer a negligible aspect. Showing the capacitance node's role is an exemplification, in this paper, of the challenges that modellers may face when using legacy software tools in simulating a system that was not originally meant to be simulated with those tools. We do not claim that this particular instance is the only, nor maybe the single most influential source that explains discrepancies between simulations and experiments. However, this example was relatively easy to demonstrate through IDA ICE (that allows users to input the value of the glass-pane material's specific heat capacity while the other tools do not allow this parameter to be modified) by comparing a simulation with and without glass's specific heat capacity. Many other possible causes cannot be so easily tested with BES tools, as there are intrinsic limitations to do so in the tools' structures.

Table 10
Energy performance of the different tools in the four analysed periods.

	Total Energy [kWh/m^2]			
Season	Winter		Summer	
Shading	ON	OFF	ON	OFF
Measured	2.8	6.3	2.4	5.4
EnergyPlus AW	3.1	8.4	2.2	6.9
TRNSYS	3.2	7	2.1	5.8
IDA ICE VW	3.8	8.1	2.8	7.8
IES-VE	N.A.	N.A.	N.A.	N.A.

The shading device's presence does not dramatically affect the tools' performance. This may be because when mechanically ventilated cavities are modelled, the influence of the heat released to the airflow on the determination of the actual air mass rate is neglected. If this assumption can be valid for wide cavities with high airflow rate, in the case of narrow cavities characterised by relatively slow (forced) airflows, such an effect might be not negligible. Improved models and modelling approaches for DSF in BES tools should, therefore, include the possibility better to specify the position of the in-cavity shading device and account for its influence on the airflow rates. So far, only IDA ICE allows specifying the shading position with respect of the cavity, while in the other tools, the shading device is assigned to the window or in a fixed position (Energy Plus) or just specifying if it is an internal or external shading. TRNSYS does not permit defining the shading position but accounts for an additional convection fraction to the zone's air node.

The tools' convection algorithms seem to have a minimal effect on the prediction of the DSF's thermophysical quantities that we used to assess the tools' reliability. It was noticed that, in IDA ICE, when modelling the façade with the zonal approach, the convection heat transfer coefficients for the cavity surfaces can assume values up to ten times higher than those obtained when modelling the same façade with the in-built model. This is because the CDA method used in the zonal approach is a function of the air change rate, which increases due to partitioning the cavity into many stacked zones. The higher the number of zones, the higher this value is [44]. Conversely, Energy Plus (zonal approach) and Trnsys use values of the same magnitude as the in-built model of IDA ICE. Moreover, it is interesting to highlight that both in IDA ICE and in Energy Plus, when the algorithm had to choose between the natural or forced convection calculation method, the natural convection coefficient was chosen. In IDA ICE, this choice was done by choosing the highest value between the two (see Table 4). In Energy Plus, the algorithm runs a series of "if … else" checks to select the calculation method. One of the conditions to use the forced convection coefficient is to have an active HVAC system present in the zone, and this led to the natural convection coefficient being adopted for all the cavity zones. Unfortunately, extracting this information for all the models was impossible (for example, the in-built model of Energy Plus and the IES VE zone-model do not output these quantities), and this limits the possibility to perform a more systematic investigation on the role of these quantities in relation to the tool's performance.

5. Conclusion

Modelling a double-skin façade is not a trivial task, and the reliability of the modelling approaches adopted in building energy simulation (BES) tools need to be verified and validated to build trust in the use of BES programs to simulate DSFs. Four different building energy simulation (BES) tools were tested against experimental data. The accuracy in predicting four physical quantities was evaluated, namely the air gap temperature, the inner glazing surface temperature, the heat flux, and the transmitted solar irradiance.

Three of these tools (EnergyPlus, IDA ICE and Trnsys) offer the modellers the possibility to approach a DSF in two ways: to use the in-built model for the DSF or develop a so-called 'zonal approach'. The two approaches were compared against experiment data, and in two out of three tools, the in-built model was the most accurate in predicting the chosen parameters. In TRNSYS the zonal approach gave better results, whilst in IES VE, it was the only model available. Therefore, the multi-software comparison was carried out by comparing two in-built models ("Airflow window" in EnergyPlus and "Ventilated window" in IDA ICE) and two zones models (TRNSYS and IES VE).

It is not straightforward to identify a tool that is able to predict all the variables in all the conditions with the same accuracy. TRNSYS appeared to be the better performing software when studying the heat flux through the component; thus, it is a more reliable tool if the simulation's goal is the energy balance over a certain amount of time. There is no

Table 11
NMBE and CV(RMSE) values calculated for the energy performance of each tool.

Season	Winter				Summer			
Shading	ON		OFF		ON		OFF	
	NMBE [%]	*CV(RMSE) [%]*	*NMBE [%]*	*CV(RMSE) [%]*	*NMBE [%]*	*CV(RMSE) [%]*	*NMBE [%]*	*CV(RMSE) [%]*
EnergyPlus AW	*14*	*52*	*32*	*77*	*−9*	*66*	*27*	*60*
TRNSYS	*15*	*72*	*11*	*35*	*−13*	*75*	*6*	*55*
IDA ICE VW	*38*	*68*	*29*	*125*	*16*	*38*	*43*	*110*
IES-VE	*N.A.*	*N.A.*	*N.A.*	*N.A.*	*N.A.*	*N.A.*	*N.A.*	*N.A.*

consistency of accurate or inferior predictions related to a specific period, and as a general trend, the winter conditions are not predicted more accurately than the summer ones. The same type of conclusion is valid for the presence of the shading device in the cavity.

BES tools may be acceptable for predicting the overall performance of a façade in terms of energy gain and loss over a certain, rather long period (e.g. a week), and the expected accuracy of the prediction is in line with the general one for BES tools. The capability of the analysed tools to predict the short-term dynamic of a DSF accurately is instead questionable due to the complex behaviour of a DSF system and the limited representation of these systems in the BES tools. Relatively large errors are observed on individual thermophysical quantities that might be used to take important decisions in the design process. The use of BES tools in sizing the systems based on typical or design days might also lead to substantial inaccuracies and should be therefore carried out in combination with other, more detailed simulation approaches. Therefore such predictions should always be either verified through experimental data or carried out with more accurate modelling strategies (e.g. on-purpose codes, CFD codes). Ad-hoc developed simulation codes or detailed CFD models can also make it possible to systematically test, verify, and quantify the impact of the different simplifications, including, for example, more in-depth analysis on the effects of the empirical correlations for calculating the convective heat transfer coefficient – something that is difficult to be done with BES tools because of intrinsic limitations that these simulation environments present.

Declaration of competing interest

None.

Acknowledgements

The authors would like to thank the researchers and technical staff from Politecnico di Torino in Italy involved in the experimental activity, which provided the data used for model validation in this study.

Part of the activities presented in this paper were carried out within the research project “REsponsive, INtegrated, VENTilated - REINVENT – windows”, supported by the Research Council of Norway through the research grant 262198, and partners SINTEF, Hydro Extruded Solutions, Politecnico di Torino, Aalto University.

The activities presented in this paper have also been supported by the ÚNKP-18-3 New National Excellence Program of the Ministry of Human Capacities of Hungary.

Appendix A

Measured quantities

In this section, the measured quantities used for the validation process are shown. The airgap and surface temperature are plotted against the transmitted solar radiation (Fig. A.1). In Fig. A.2 , heat flux is plotted against the transmitted solar radiation.

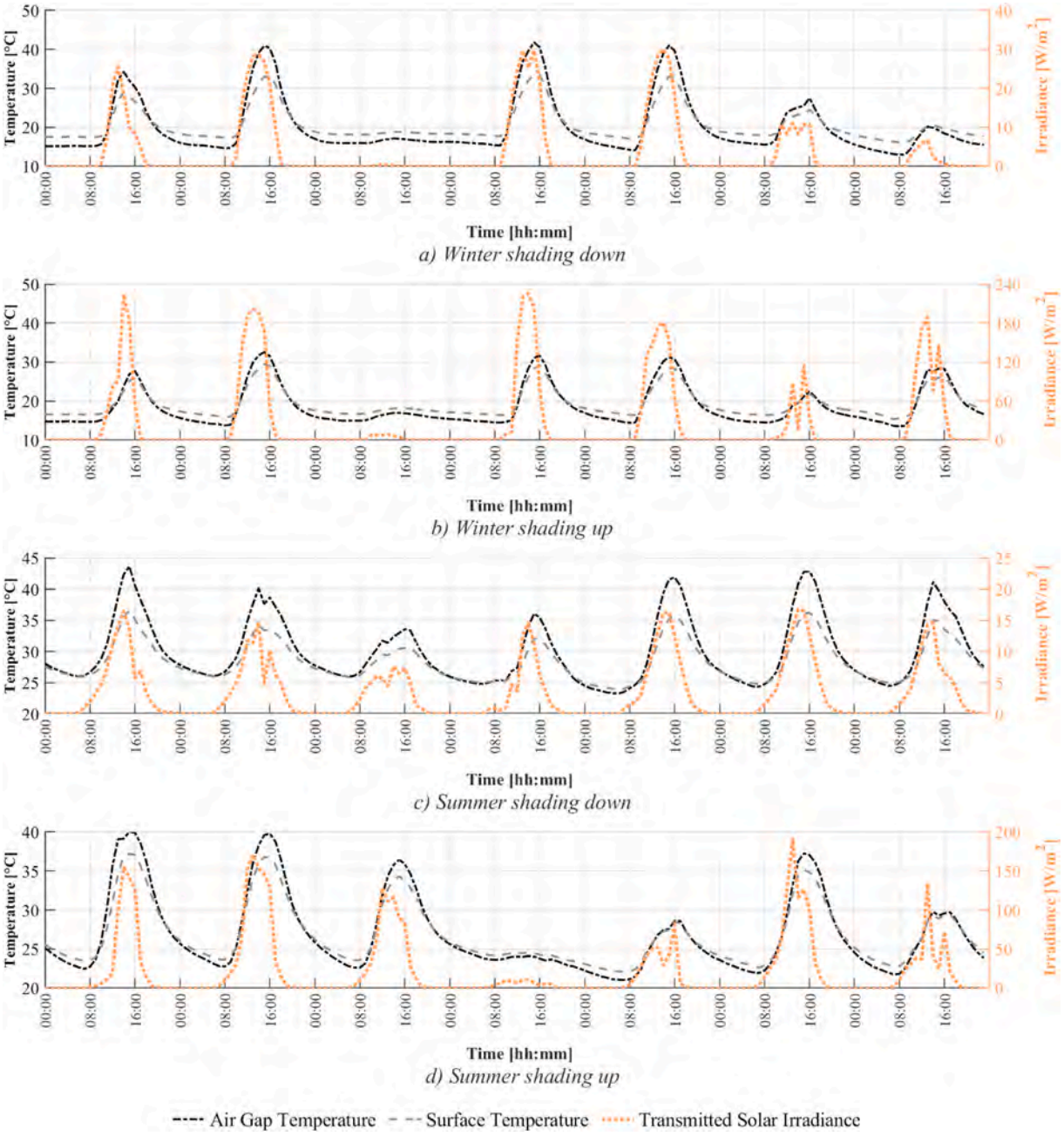

Fig. A1. Time profile of the air gap and the indoor surface temperature [°C] and the transmitted solar irradiance [W/m^2] for the four modelling periods: a) Winter with shading down, b) Winter with shading up, c) Summer with shading down and d) Summer with shading up.

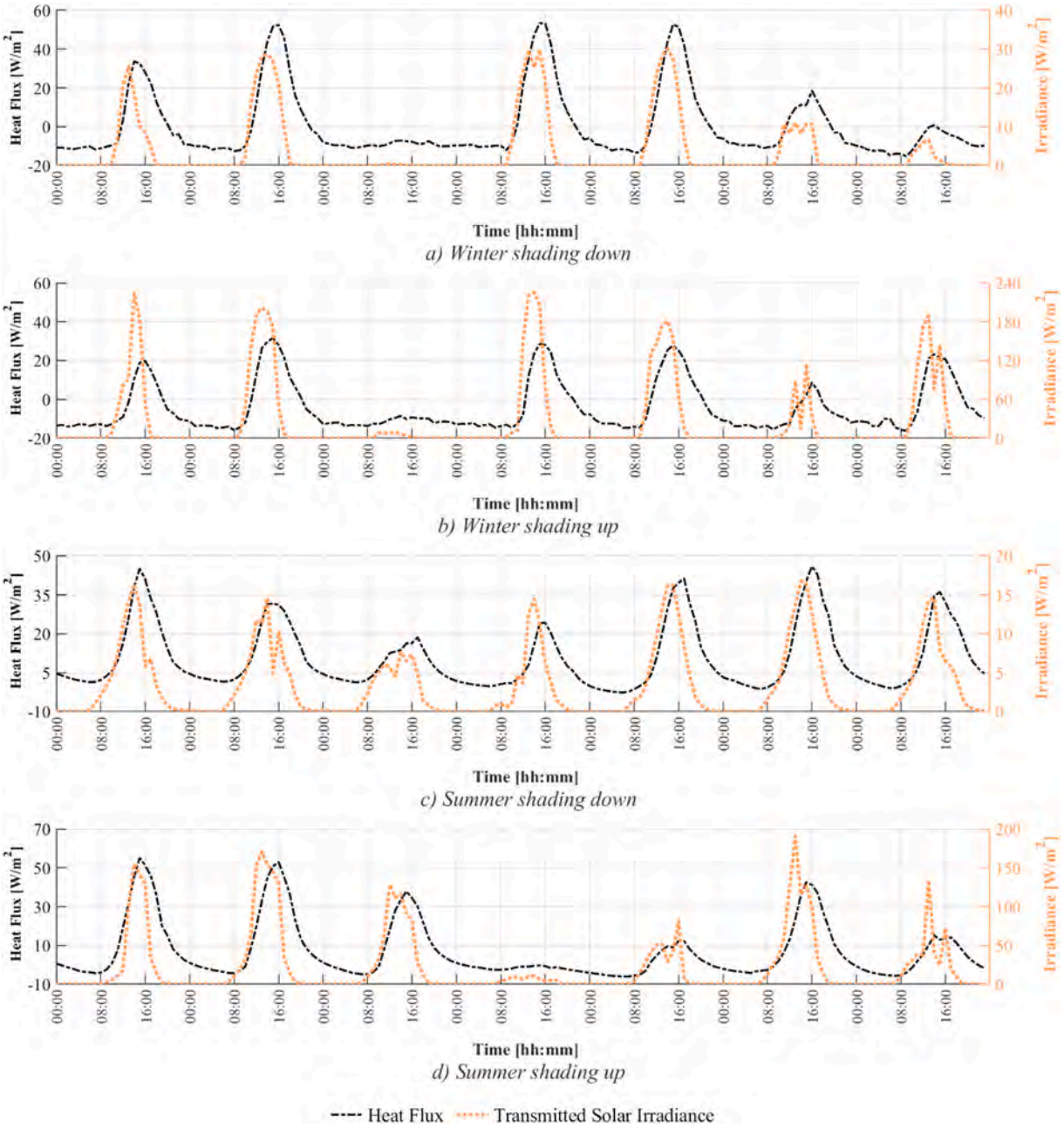

Fig. A2. Time profile of the heat flux and the transmitted solar irradiance [W/m^2] for the four modelling periods: a) Winter with shading down, b) Winter with shading up, c) Summer with shading down and d) Summer with shading up.

Appendix B

Modelling of DSF in EnergyPlus

EnergyPlus allows the modelling a DSF by using an in-built component, called *"Airflow Window"*, or through the implementation of the modelling strategies based on stacked thermal zones, and both methods were tested in this investigation.

In-built model: "Airflow window"

One of the two models of the DSF has been carried out by using the in-built component "*Airflow Window*" (as implemented in EnergyPlus 9.1). This component only allows to model mechanically ventilated windows, and it can run in five different configurations, among which the "Air exhaust" mode [62], which is the one we selected to replicate the climate façade configuration. In this modelling approach, the inlet air to the façade is taken from the indoor air node of the thermal zone to which the DSF is associated, while the exhausted air is linked directly to the outdoor air node.

In general, the software allows the modeller to specify the characteristics of a window construction pane by pane, with a limitation of maximum eight layers in the construction (including glass panes, cavities, and shading) by making use of the conventional features available in EnergyPlus for the modelling of glazing systems. The shading device was modelled as "Between glass shade". The shading device's position cannot be specified, and by default, it is set in the middle of the cavity. It can be controlled through a schedule – following the usual control possibilities for shading devices for

any other conventional window systems in EnergyPlus. When the shading device is deployed, the ventilated cavity results divided into two equal sub-cavities that are crossed by the same airflow rate, which is half of the value provided for the entire cavity. The modeller inputs the nominal (maximum) airflow rate that crosses the ventilated window and the airflow rate can be controlled through a dedicated schedule in the range 0–100%. When set to 0%, the airflow window is operated as a non-ventilated window. No information is required on the fans to mechanically extract the air from the ventilated cavity as these are, in practice, not modelled, and the airflow rate occurring in the cavity is always equivalent to that given through the schedule. The correlation of the heat convection coefficient for the ventilated cavity cannot be chosen or overrode. The in-built model adopts the calculation method detailed in ISO 15099 [50]. It is a function of the air velocity and the convective coefficient calculated for an enclosed gap (Table 4).

Zonal model

The other model implemented in EnergyPlus was obtained by modelling the façade as three stacked thermal zones. Each zone was modelled with an exterior double glazing, an interior single glazing and the opaque surfaces facing the exterior set as adiabatic. The surface between each stack zone is modelled as a window made of infrared transparent material.

The airflow between the occupied zone and the façade zones was modelled utilising the 'Airflow Network'. It consists of a set of nodes corresponding to each zone and the outdoor environment which are linked by airflow components. An effective leakage area (ELA) corresponding to the window opening was used for connecting the occupied zone to the façade bottom zone. The stacked zones of the façade are linked, employing a horizontal opening always open. An exhaust fan was used to connect the top zone of the façade to the exterior. The nodes' variable is the pressure, and the linkage's variable is the airflow rate. Newton's method is used to solve for node air pressures. The pressure difference across each linked component is assumed to be governed by Bernoulli's equation. Internal solar radiation distribution was calculated using the "full interior and exterior" mode. This calculation mode tracks the amount of radiation that reaches each zone's surface by projecting direct solar radiation through the exterior window into the internal surfaces. Wind data were not available from the experimental data, and being the façade running in a mechanical configuration, the influence of the wind can be disregarded. Therefore, the model did not account for wind pressure.

The convection coefficients for the cavity surfaces are chosen by the 'adaptive algorithm'. The adaptive convection algorithm is based on classifying surfaces by flow regime and orientation so that the correct h_c equation can be chosen at a particular point in time during the simulation. The correlations available for the window's surfaces are shown in Table 4. If the flow regime is 'natural' the h_c is calculated according to the ISO 15099 [50]; if the flow regime is forced, the Goldstein Novoselac Ceiling Diffuser Window correlation is adopted [51]. Selecting the flow regime is done according to the HVAC (element type, operating status and ACH). Though, in the thermal zones of the DSF, no HVAC element is present in the zone itself; therefore, the algorithm always chooses the natural convection correlation.

Modelling of DSF in IDA ICE

The models were developed by using IDA ICE 4.8 (SP1). There are two main approaches for modelling DSFs within the tool:

- the in-built component (ventilated window model, *vw*)
- or the façade can be constructed tailor-made consisting of one or more connected thermal zones.

In-built model: "ventilated window model"

The *vw model* consists of two detailed window models representing the two transparent skins, with the possibility to model the shading on either side of the two windows. The detailed window model makes a layer by layer computation of multiple reflections, and each layer temperature is computed, following the modelling procedure presented in the ISO 15099 [50]. The detailed window model also includes a capacity node for the glazing and the shading [63].

The ventilated window model allows implementing the cavity's inlets and outlets both towards the internal and external environment, as well as connection to the HVAC system. A window opening toward the cavity can also be defined. No enclosing elements around the cavity are considered in the calculation, except for the façade elements (glazing, frames, shading) parallel to the façade [64]. Averaged cavity-air temperatures are calculated based on the inlet temperature, mass flow and solar energy and heat transferred through the surfaces. Wind and buoyancy-driven airflows through leaks and openings can be calculated via a fully integrated airflow network model [65].

The shading layer was modelled as part of the exterior window, and it was modelled as an interior shade. Its distance was defined as measured from the external skin and set as in the experimental setup. A schedule controlled the shading's presence inside the cavity. The inlet from the indoor environment was modelled as a leak while the exhaust fan was modelled as an idealised exhaust terminal, which works as ON/OFF fan controlled by a schedule. The modeller inputs the nominal minimum and maximum airflow rate that crosses the façade, and the mass flow is controlled within that range. If the fan is ON, the airflow is the nominal maximum airflow rate. If the fan is set to OFF, the fan behaves as a leak and adopts the nominal minimum airflow rate. This value cannot be set to zero.

The convection coefficients for the indoor surfaces of the DSF are calculated choosing the greater of two methods (natural and forced airflow) calculated for each skin, regardless of the actual main driving force in the model (Table 4).

Zonal model

The DSF can also be modelled by constructing an airflow network across a series of thermal zones. The zonal model was done using three stacked zones, defining the geometry, material and openings towards the cavity through the graphical interface. The inlet to the façade was modelled as a large vertical opening with two-way flows, set as always open by mean of a schedule. The stacked zones' connection was then developed by using the advanced modelling approach.

The zones' horizontal partitions could not be modelled as transparent openings in the graphic model. The reason for this was that the surface of these partitions (0.352 m^2) was too small for the software tool to recognise them as a partitioning element (walls, ceilings, and floors that are smaller than 0.5 m^2 will be ignored in the model) which, on the one hand, caused that the partition surfaces were modelled as adiabatic surfaces, not connected with each other; on the other hand, made it impossible to add windows or openings within these partitions using the graphical interface [65]. To account for the solar radiation through horizontal openings, an element for the light distribution calculation between the surfaces in the zone is

needed (called RAY). Each surface that collaborates in the light distribution (window or opening) undergoes several coordinate transformations in order to be used in the RAY element, hence modifying and extending this set of data was a too complex task, not viable during a standard design project. Therefore each opening that was not automatically created through the graphic interface was modelled as only including the airflow connections, as a large horizontal rectangular opening with two-way flows. The solar radiation transmitted through the façade partitions was hence discarded, but the radiation was absorbed and reflected back to the zone in an equal portion ($r = 0.5$).

The exhaust from the façade was modelled connecting an exhaust fan to the cavity's top zone. As in the inbuilt model, the element used was an idealised exhaust terminal. Moreover, similarly to the in-built model, the shading layer was modelled as part of the external window. Hence the external cavity was not part of the airflow network. This approach simplifies the airflow patterns seen in reality (e.g. Ref. [66]), where both cavities are ventilated to some extent.

The default settings were used for the convection calculation method of the cavity thermal zone inner surfaces; the zone model uses the greater between the CDA (Ceiling Diffuser Algorithm - a function of air change rate), and the method of Brown & Isfält [52], which between predefined table values as a function of the temperature difference of the surface and the air (Table 4).

Modelling of DSF in IES VE

The model was created employing IES VE 2019. The modelling of the double-skin façade was obtained using different stacked thermal zones. The module '*Apache*' was used to assign the building's thermal properties; '*ApacheHVAC*' was used to model the AHU and the extraction fans; the '*MacroFlo*' module was used to model the openings (inlet and horizontal partitions) and the airflow through them. The occupied zone was created with five surfaces with adjacent surface temperature assigned by a schedule. The temperature inside the zone was also controlled to reach the experiment measured temperature, which was achieved utilising an AHU equipped with electric cooling and heating coils. In order to assign values from a schedule, an external module '*Ergon*' was adopted to couple the IES model. The façade was modelled as three equal stacked zones, as explained in the previous paragraphs. The horizontal partitions were modelled as horizontal windows and then set as 'holes'. Holes are entirely transparent to solar radiation, and MacroFlo treats them as open to the passage of air. The inlet opening area was set as a percentage of the bottom zone's internal glazing. An exhaust fan was applied to the top zone of the DSF to provide the requested airflow through the façade. The connection between the HVAC system's thermal zones was done by defining each stacked zone as a 'Room Component' in the ApacheHVAC module. The airflow extracted by the fan was controlled by a time switch that allowed controlling the nominal airflow and if the fan was ON or OFF. The airflow was set to a constant value and always ON. The shading device (blind) is assigned to the internal side of the external glazing system; it is not possible to define the distance from the glass.

The simulation engine 'ApacheSim' determines the building's thermal conditions by balancing sensible and latent heat flows, entering and leaving each air mass and each building surface. ApacheSim uses a stirred tank model of the air in a room. Since ApacheHVAC and MacroFlo are included, the calculations also include the mechanical and natural ventilation airflow rates calculated by these tools and the inter-dependence between these variables and those calculated within ApacheSim.

The building's inner surfaces' convection coefficient, including the DSF ones, is calculated using the Alamdari and Hammond's correlation [48].

Modelling of DSF in TRNSYS

The models were developed by using Trnsys17 and Trnsys18. There are two main approaches for modelling DSFs within the tool:

- the in-built component (complex fenestration system, *CFS – only available in version 18*)
- or the façade can be constructed tailor-made consisting of one or more connected thermal zones (it is possible to implement this approach in any version of the tool, in this paper, version 17 was used).

In-built model: "complex fenestration system"

In this work, TRNSYS (version 18) was used. The new version of the multi-zone building model Type 56 enables a detailed CFS simulation, which among other features, allows modelling mechanically ventilated gaps. Data for both models were defined through the interface TRNBuild. A single thermal zone with two windows was modelled in TRNSYS 3D Building plug-in for SketchUp. This plug-in allows defining the geometry and the boundary conditions. The glazing's thermal and optical properties were prior defined in Window 7.7. For every glazing/shading configuration, the BSDF matrixes (transmission front/back, reflection front/back and absorption per layer) was generated beforehand for the whole system in the solar and visual band. The BSDF matrixes were combined into one external file, which was imported by Type 56 during the initializing step. A specific standard created by Transso-lar is necessary to create a readable file by Type 56.

The position of the shading in the cavity is also defined in Window. It can be controlled through a schedule – following the usual control possibilities for shading devices.

The component allows to model only mechanically ventilated cavities. It is necessary to define the airflow in two cavities; during the export phase, the cavity is automatically divided into two equally wide cavities in order to model the configuration without the shading. When the shading is deployed, the two cavities have the dimensions defined in the Window 7 model. Thus, the mass flow was distributed 50/50 in the case of no shading and proportionally to the cavity width when there is the blind. The component requires setting the inlet air temperature (fixed value or a schedule), which in this case it is assumed to be equal to the zone air temperature. The model does not require any modelling of the inlet or outlet opening. The façade is modelled as an exhaust façade by choosing to transfer the convective heat flow extracted from the cavity to the outside node's cavity.

No information is required on the fans to mechanically extract the air from the ventilated cavity as these are, in practice, not modelled, and the airflow rate occurring in the cavity is always equivalent to that given value. The correlation of the heat convection coefficient for the ventilated cavity cannot be chosen or overrode. The in-built model adopts the calculation method detailed in ISO 15099 [50,67]. It is a function of the air velocity and the convective coefficient calculated for an enclosed gap (Table 4).

Zonal model

In this work, TRNSYS (version 17) was used with TNRFLOW (version 1.4), a modified version of the multi-zone building model Type 56, which

integrates the multi-zone airflow model COMIS. Data for both models were defined through the interface TRNBuild. The model geometry was defined in the TRNSYS 3D Building plug-in for SketchUp. This plug-in allows defining three zones stacked on top of each other and the adjoining room, to define boundary conditions and perform surface matching between zones. The horizontal openings were modelled as 'virtual surface', and this allowed to maintain three coupled air nodes once that the model is imported into the TRNBuild interface; in fact, the three stacked zones were merged into one thermal (radiative) zone with three air nodes at different heights. The airflow network interacts with air nodes, whereas the radiation balance is solved for thermal zones [68].

Both the air inlet and outlet to the cavity were modelled as a circular duct set to equal the experiment's opening size, and the extraction fan (connected to the outlet node) was modelled as a constant flow fan with a constant pressure curve. To connect the cavity air nodes, horizontal openings (large openings with zero height) matching the cavity dimensions were used.

By using 3D-geometry, models of short-wave direct and diffuse solar irradiance are made available to distribute solar gains entering zones through external glazing [69]. These features allowed for a detailed distribution of direct and diffuse radiation, including multiple reflections in the merged cavity zone. In the zone representing the office space, where solar radiation is only entering through adjacent windows, surface shading and solar gains distribution are simplified. In this case, the default surface distribution factors (for walls, floor and ceiling) were left unchanged. According to the software documentation, the detailed models for direct and diffuse radiation are recommended for highly glazed zones like atriums and DSFs where the distribution of solar radiation is critical but will have a lower impact on the results when shading devices are activated [33].

The shading was assigned to the external glazing layer as an interior shading device. Its position cannot be defined, but a simple fraction of additional convection to the air node can be specified instead. The amount of solar radiation absorbed by the internal shading device that is transferred to the air node by additional convection (between the inner layer pane and the internal shading device) will depend not only on the distance to the shading device but the type and height of the shading device, the geometry of the air volume between the shading device and the glazing and the actual surface and air temperatures. According to the software documentation, a value of zero represents an internal shading device located very close to the pane without any airflow in between. Typical values range between 0.3 and 0.6, and the default value of 0.5 was therefore used.

The convective coefficient of the inner surfaces of the DSF is calculated adopting the internal calculation method (Table 4), while for all the other surfaces, a default fixed value is assigned.

Public availability of models for the different software tools

In an effort to make our research freely accessible and to allow easy replication of our results, we make available, on an open-access repository, the models developed with the different simulation environments for this study. These can be found at, and referenced using, the following https://doi.org/10.5281/zenodo.4573644 [70].

References

[1] V. Huckemann, E. Kuchen, M. Leão, É.F.T.B. Leão, Empirical thermal comfort evaluation of single and double skin façades, Build. Environ. 45 (2010) 976–982, https://doi.org/10.1016/j.buildenv.2009.10.006.

[2] F. Pomponi, P.A.E. Piroozfar, R. Southall, P. Ashton, E.R.P. Farr, Energy performance of Double-Skin Façades in temperate climates: a systematic review and meta-analysis, Renew. Sustain. Energy Rev. 54 (2016) 1525–1536, https://doi.org/10.1016/j.rser.2015.10.075.

[3] C.S. Park, G. Augenbroe, T. Messadi, M. Thitisawat, N. Sadegh, Calibration of a lumped simulation model for double-skin façade systems, Energy Build. 36 (2004) 1117–1130, https://doi.org/10.1016/j.enbuild.2004.04.003.

[4] C.S. Park, G. Augenbroe, N. Sadegh, M. Thitisawat, T. Messadi, Real-time optimization of a double-skin façade based on lumped modeling and occupant preference, Build. Environ. 39 (2004) 939–948, https://doi.org/10.1016/j.buildenv.2004.01.018.

[5] Y. Wang, Y. Chen, J. Zhou, Dynamic modeling of the ventilated double skin façade in hot summer and cold winter zone in China, Build, Environ. Times 106 (2016) 365–377, https://doi.org/10.1016/j.buildenv.2016.07.012.

[6] Y. Li, J. Darkwa, G. Kokogiannakis, Heat transfer analysis of an integrated double skin façade and phase change material blind system, Build. Environ. 125 (2017) 111–121, https://doi.org/10.1016/j.buildenv.2017.08.034.

[7] A. Dama, D. Angeli, O. Kalyanova Larsen, Naturally ventilated double-skin façade in modeling and experiments, Energy Build. 114 (2017) 17–29.

[8] D. Saelens, S. Roels, H. Hens, Strategies to improve the energy performance of multiple-skin facades, Build. Environ. 43 (2008) 638–650, https://doi.org/10.1016/j.buildenv.2006.06.024.

[9] N.M. Mateus, A. Pinto, G.C. Da Graça, Validation of EnergyPlus thermal simulation of a double skin naturally and mechanically ventilated test cell, Energy Build. 75 (2014) 511–522, https://doi.org/10.1016/j.enbuild.2014.02.043.

[10] F. Pomponi, S. Barbosa, P.A.E. Piroozfar, On the intrinsic flexibility of the double skin façade: a comparative thermal comfort investigation in tropical and temperate climates, Energy Procedia 111 (2017) 530–539, https://doi.org/10.1016/j.egypro.2017.03.215.

[11] A. Gelesz, Á. Bognár, A. Reith, Effect of shading control on the energy savings of an adaptable ventilation mode double skin facade, in: 13th Conf. Adv. Build. Ski. 1-2 Oct. 2018, Bern, Switz. - Prog., 2018.

[12] Z. Eskinja, L. Miljanic, O. Kuljaca, Modelling thermal transients in controlled double skin Façade building by using renowned energy simulation engines, in: 2018 41st Int. Conv. Inf. Commun. Technol. Electron. Microelectron. MIPRO 2018 - Proc., 2018, pp. 897–901, https://doi.org/10.23919/MIPRO.2018.8400166.

[13] D. Kim, S.J. Cox, H. Cho, J. Yoon, Comparative investigation on building energy performance of double skin façade (DSF) with interior or exterior slat blinds, J. Build. Eng. 20 (2018) 411–423, https://doi.org/10.1016/j.jobe.2018.08.012.

[14] E. Taveres-Cachat, F. Favoino, R. Loonen, F. Goia, Ten questions concerning co-simulation for performance prediction of advanced building envelopes, Build. Environ. (2021), 107570, https://doi.org/10.1016/j.buildenv.2020.107570.

[15] M. Haase, F. Marques da Silva, A. Amato, Simulation of ventilated facades in hot and humid climates, Energy Build. 41 (2009) 361–373, https://doi.org/10.1016/j.enbuild.2008.11.008.

[16] C. Tabares-Velasco, P.C. Christensen, M. Bianchi, Verification and validation of EnergyPlus phase change material model for opaque wall assemblies, Build. Environ. 54 (2012) 186–196, https://doi.org/10.1016/j.buildenv.2012.02.019.

[17] M. Barclay, N. Holcroft, A.D. Shea, Methods to determine whole building hygrothermal performance of hemp-lime buildings, Build. Environ. 80 (2014) 204–212, https://doi.org/10.1016/j.buildenv.2014.06.003.

[18] R.H. Henninger, M.J. Witte, D.B. Crawley, Analytical and comparative testing of EnergyPlus using IEA HVAC BESTEST E100-E200 test suite, Energy Build. 36 (2004) 855–863, https://doi.org/10.1016/j.enbuild.2004.01.025.

[19] J. Neymark, R. Judkoff, G. Knabe, H.-T. Le, M. Dürig, A. Glass, G. Zweifel, Applying the building energy simulation test (BESTEST) diagnostic method to verification of space conditioning equipment models used in whole-building energy simulation programs, Energy Build. 34 (2002) 917–931, https://doi.org/10.1016/S0378-7788(02)00072-5.

[20] E. Catto Lucchino, F. Goia, G. Lobaccaro, G. Chaudhary, Modelling of double skin facades in whole-building energy simulation tools: a review of current practices and possibilities for future developments, Build. Simul. 12 (2019) 3–27, https://doi.org/10.1007/s12273-019-0511-y.

[21] O. Kalyanova, P. Heiselberg, C. Felsmann, H. Poirazis, P. Strachan, A. Wijsman, An empirical validation of building simulation software for modelling of doubleskin facade (DSF), in: Elev. Int. IBPSA Conf., Glasgow, Scotland, 2009.

[22] A. Gelesz, E. Catto Lucchino, F. Goia, A. Reith, V. Serra, Reliability and sensitivity of building performance simulation tools in simulating mechanically ventilated double skin facades, in: V. Corrado, A. Gasparella (Eds.), Proc. Build. Simul. 2019 16th Conf, IBPSA, Rome, 2019.

[23] Energy Plus, EnergyPlus 9.1 Engineering Reference: the Reference to EnergyPlus Calculations, 2019, pp. 1–847, doi.org/citeulike-article-id:10579266.

[24] V.M. Soto Francés, E.J. Sarabia Escriva, J.M. Pinazo Ojer, E. Bannier, V. Cantavella Soler, G. Silva Moreno, Modeling of ventilated façades for energy building simulation software, Energy Build. 65 (2013) 419–428, https://doi.org/10.1016/j.enbuild.2013.06.015.

[25] D.-W. Kim, C.-S. Park, Difficulties and limitations in performance simulation of a double skin façade with EnergyPlus, Energy Build. 43 (2011) 3635–3645, https://doi.org/10.1016/j.enbuild.2011.09.038.

[26] W. Choi, J. Joe, Y. Kwak, J.H. Huh, Operation and control strategies for multi-storey double skin facades during the heating season, Energy Build. 49 (2012) 454–465, https://doi.org/10.1016/j.enbuild.2012.02.047.

[27] N. Papadaki, S. Papantoniou, D. Kolokotsa, A parametric study of the energy performance of double-skin façades in climatic conditions of Crete, Greece, Int. J. Low Carbon Technol. 9 (2013) 296–304, https://doi.org/10.1093/ijlct/cts078.
[28] A.S. Anđelković, I. Mujan, S. Dakić, A.S. Anđelković, I. Mujan, S. Dakić, Experimental validation of a EnergyPlus model: application of a multi-storey naturally ventilated double skin façade, Energy Build. 118 (2016) 27–36, https://doi.org/10.1016/j.enbuild.2016.02.045.
[29] A.B. Equa, IDA Indoor Climate and Energy 4.0 EQUA Simulation AB, 2009.
[30] E. Colombo, M. Zwahlen, M. Frey, J. Loux, Design of a glazed double-façade by means of coupled CFD and building performance simulation, Energy Procedia 122 (2017) 355–360, https://doi.org/10.1016/j.egypro.2017.07.337.
[31] V.E. Ies, ApacheSim User Guide, IES VE User Guid, 2014.
[32] E.A. Pekdemir, R.T. Muehleisen, A parametric study of the thermal performance of double skin façades at different climates using annual energy simulation, Fifth Natl. Conf. IBPSA, 2012, pp. 211–218, https://doi.org/10.1016/j.ijrobp.2008.07.056.
[33] Trnsys 17, Multizone Building modeling with Type56 and TRNBuild 5 (2013) 1–79.
[34] D. Saelens, S. Roels, H. Hens, The inlet temperature as a boundary condition for multiple-skin facade modelling, Energy Build. 36 (2004) 825–835, https://doi.org/10.1016/j.enbuild.2004.01.005.
[35] U. Eicker, V. Fux, U. Bauer, L. Mei, D. Infield, Facades and summer performance of buildings, Energy Build. 40 (2008) 600–611, https://doi.org/10.1016/j.enbuild.2007.04.018.
[36] F.P. López, R.L. Jensen, P. Heiselberg, M. Ruiz de Adana Santiago, Experimental analysis and model validation of an opaque ventilated facade, Build. Environ. 56 (2012) 265–275, https://doi.org/10.1016/j.buildenv.2012.03.017.
[37] C. Aparicio-Fernández, J.L. Vivancos, P. Ferrer-Gisbert, R. Royo-Pastor, Energy performance of a ventilated façade by simulation with experimental validation, Appl. Therm. Eng. 66 (2014) 563–570, https://doi.org/10.1016/j.applthermaleng.2014.02.041.
[38] H. Elarga, A. Zarrella, M. De Carli, Dynamic energy evaluation and glazing layers optimization of façade building with innovative integration of PV modules, Energy Build. 111 (2016) 468–478, https://doi.org/10.1016/j.enbuild.2015.11.060.
[39] I. Khalifa, L.G. Ernez, E. Znouda, C. Bouden, Coupling TRNSYS 17 and CONTAM: simulation of a naturally ventilated double-skin facade, Adv. Build. Energy Res. 9 (2015) 293–304, https://doi.org/10.1080/17512549.2015.1050694.
[40] I. Khalifa, L. Gharbi-Ernez, E. Znouda, C. Bouden, Assessment of the inner skin composition impact on the double-skin façade energy performance in the mediterranean climate, Energy Procedia 111 (2017) 195–204, https://doi.org/10.1016/j.egypro.2017.03.021.
[41] M. Shahrestani, R. Yao, E. Essah, L. Shao, A.C. Oliveira, A. Hepbasli, E. Biyik, T. del Cano, E. Rico, J.L. Lechòn, Experimental and numerical studies to assess the energy performance of naturally ventilated PV facade systems, Sol. Energy 147 (2017) 37–51, https://doi.org/10.1016/j.solener.2017.02.034.
[42] M. Hiller, J. Merk, P. Schöttl, Complex Fenestration Systems Tutorial, 2017, pp. 1–22.
[43] V. Leal, E. Erell, E. Maldonado, Y. Etzion, Modelling the SOLVENT ventilated window for whole building simulation, Build. Serv. Eng. Technol. 25 (2004) 183–195, https://doi.org/10.1191/0143624404bt103oa.
[44] A. Gelesz, Sensitivity of exhaust-air façade performance prediction to modelling approaches in IDA ICE, Int. Rev. Appl. Sci. Eng. 10 (2019) 241–252.
[45] J.A. Clarke, Energy Simulation in Building Design, Adam Hilger Ltd., Bristol & Boston, 1985.
[46] A.B. Equa Simulation, IDA Indoor Climate and Energy [Computer Software] Version: 4.8 SP1, 2018.
[47] W.H. McAdams, Heat Transmission, McGraw-Hill, Kogakusha, Tokyo, Japan, 1954.
[48] F. Alamdari, G. Hammond, Improved data correlation for buoyancy-driven convection in rooms, Build. Serv. Eng. Technol. 4 (1983) 106–112.
[49] TRNSYS 17, mathematical reference, TRNSYS Doc 4 (2009) 1–486.
[50] International Organisation for Standardisation, ISO 15099:2003 Thermal Performance of Windows, Doors and Shading Devices - Detailed Calculations, 2003.
[51] K. Goldstein, A. Novoselac, Convective heat transfer in rooms with ceiling slot diffusers (rp-1416), HVAC R Res. 16 (2010) 629–655, https://doi.org/10.1080/10789669.2010.10390925.
[52] G. Brown, E. Isfält, Solinstrålning Och Solavskärmning (Solar Irradiation and Sun Shading Devices) - Report 19, 1974. Stockholm.
[53] VDI Heat Atlas, 2010, https://doi.org/10.1007/978-3-540-77877-6.
[54] F. Goia, V. Serra, Analysis of a non-calorimetric method for assessment of in-situ thermal transmittance and solar factor of glazed systems, Sol. Energy 166 (2018) 458–471, https://doi.org/10.1016/j.solener.2018.03.058.
[55] F. Goia, L. Bianco, M. Perino, V. Serra, Energy performance assessment of and advanced integrated facade through experimental data analysis, Energy Procedia 48 (2014) 1262–1271, https://doi.org/10.1016/j.egypro.2014.02.143.
[56] D.T. Reindl, W.A. Beckman, J.A. Duffie, Diffuse fraction correlations, Sol. Energy 45 (1990) 1–7, https://doi.org/10.1016/0038-092X(91)90123-E.
[57] R. Perez, R. Stewart, R. Seals, T. Guertin, The development and verification of the Perez diffuse radiation model, Sandia National Laboratories Albuquerque, New Mexico (USA), Report nr. SAND88-7030 (1988), https://doi.org/10.2172/7024029.
[58] F. Kasten, G. Czeplak, Solar and terrestrial radiation dependent on the amount and type of cloud, Sol. Energy 24 (1980) 177–189, https://doi.org/10.1016/0038-092X(80)90391-6.
[59] M. Martin, P. Berdahl, Characteristics of infrared sky radiation in the United States, Sol. Energy 33 (1984) 321–336.
[60] ASHRAE, ASHRAE Guideline 14 - Measurement of Energy, Demand, and Water Savings, 2014.
[61] T.P. Mcdowell, D.E. Bradley, M. Hiller, J. Lam, J. Merk, Trnsys 18 : the continued evolution of the software. IBPSA 2017- Proc, 15th IBPSA Conf., 2017, pp. 1922–1930.
[62] U.S. Department of Energy, Engineering Reference, 8.8, 2017.
[63] J. Hensen, M. Barták, F. Drkal, Modeling and simulation of a double-skin façade system, Build. Eng. 108 (2002) 461–471, https://doi.org/10.1197/jamia.M1103.
[64] Equa Simulation AB, IDA –Indoor Climate and Energy Ver 3.0 NMF-Model Documentation, ((n.d.)).
[65] A.B. Equa, EQUA Simulation AB User Manual IDA Indoor Climate and Energy, 2013.
[66] D. Saelens, Energy Performance Assessment of Single Storey Multiple-Skin Facades, 2002 doi.org/Ph. D. thesis.
[67] M. Hiller, P. Schöttl, MODELLIERUNG KOMPLEXER VERGLASUNGSSYSTEME IN TRNSYS, BauSIM, 2014.
[68] M. Hiller, S. Holst, T. Welfonder, A. Weber, M. Koschenz, TRNFLOW: Integration of the Airflow Model COMIS into the Multizone Building Model of TRNSYS, TRANSSOLAR Energietechnik Gmbh, 2002.
[69] J. Aschaber, M. Hiller, R. Weber, Trnsys 17: New Features of the Multizone Building Model, vol. 2009, Ipbsa, 2009, pp. 1983–1988.
[70] E. Catto Lucchino, A. Gelesz, K. Skeie, G. Gennaro, A. Reith, V. Serra, F. Goia, Models for Mechanically Ventilated Single-Story Double Skin Façade, 2021, https://doi.org/10.5281/zenodo.4573644.